Journal of High Energy Physics, Gravitation and Cosmology, 2026, 12(2), 1075-1130
https://www.scirp.org/journal/jhepgc
ISSN Online: 2380-4335
ISSN Print: 2380-4327

Effective Age of the Universe: A Relativistic Reformulation of Cosmological Dynamics

Jami Hossain

Centre for Energy, Physics, and Analytics, Gurgaon, India
Email: jami.hossain@cepaorg.net

How to cite this paper: Hossain, J. (2026) Effective Age of the Universe: A Relativistic Reformulation of Cosmological Dynamics. *Journal of High Energy Physics, Gravitation and Cosmology*, **12**, 1075-1130.
https://doi.org/10.4236/jhepgc.2026.122057

Received: December 17, 2025
Accepted: April 17, 2026
Published: April 20, 2026

Abstract

We demonstrate that the Effective Age of the Universe (EAoU) corresponds to an observer-accumulated duration of ≈46 Gyr, substantially longer than the canonical 13.8 Gyr obtained from the FLRW comoving frame. The latter represents the proper time measured along idealized comoving worldlines, whereas the effective duration arises when all past intervals are integrated in the observer's frame using the standard relativistic mapping between emission and observation intervals, $\mathrm{d}T_{\mathrm{obs}} = (1+z)\mathrm{d}t$. Within the context of post-recombination cosmological evolution, this observer-centric reformulation remains fully consistent with ΛCDM dynamics while extending the temporal budget available for early galaxy assembly, quasar growth, and supermassive black-hole formation. Using concordance cosmological parameters, the observer-frame accumulation yields EAoU, $T_{\mathrm{eff}} \approx 46.1$ Gyr (quoted as ≈46 Gyr), corresponding to a dilation factor $\kappa \approx 3.35$. The EAoU formulation is derived directly from general relativity and applied consistently across 4284 independent probes (detailed in Section 4.1), including Type Ia supernovae, gamma-ray bursts, quasars, strong-lensing time delays, galaxy and cluster chronometers, and early-galaxy/SMBH growth diagnostics. The EAoU framework may affect the interpretation of the H_0 tension by modifying the effective temporal baseline used to relate early- and late-Universe observables. Having established the EAoU framework, we further examine the pre-recombination Universe—from radiation domination and primordial nucleosynthesis to the approach toward the Planck scale—to evaluate its contribution to the observer-frame chronology. The early Universe lies at an asymptotically divergent instantaneous time-dilation factor, while the accumulated observer-frame time remains finite (≈1 Gyr), indicating that the classical Big Bang singularity acts not as a temporal boundary, but as a dilation horizon. The EAoU framework therefore provides a unified, empirically supported, and observer-anchored description of cosmic time, extending both early- and late-Universe interpretations without altering the ΛCDM

geometry or invoking new physics.

Keywords

Cosmology, Theory, Relativistic Cosmology, Cosmological Dynamics, Recombination, Cosmic Time and Chronology, ΛCDM Framework, Cosmological Time Dilation, Effective Age of the Universe (EAoU), Hubble Constant Tension, Strong-Lensing Time Delays, Type Ia Supernovae, Early Galaxy and Quasar Formation, Inflation

1. Definitions, Notations, and Key Formulae

This section collects key symbols, definitions, and notations used throughout the manuscript to provide clarity and consistency for the reader.

Fundamental Time Intervals

- $\mathrm{d}\tau_{\mathrm{com}}$: Infinitesimal proper-time interval measured along the worldline of a comoving observer.
  In the FLRW framework, $\mathrm{d}\tau_{\mathrm{com}} = \mathrm{d}t$, since cosmic time t is defined as the proper time of comoving observers.
- $\mathrm{d}\tau_{\mathrm{em}}$: Infinitesimal proper-time interval measured in the rest frame of the emitting source—*i.e.*, the local time between two successive emission events on the same physical clock.
  It is related to the cosmic coordinate time $\mathrm{d}t$ by the metric:
  $$\mathrm{d}\tau_{\mathrm{em}}^2 = g_{00}\, c^2 \mathrm{d}t^2$$
  For comoving emitters in an FLRW metric, $g_{00} = -1$, hence $\mathrm{d}\tau_{\mathrm{em}} = \mathrm{d}t$.
  For galaxies or sources comoving with the cosmic flow (no peculiar velocity), the emitter proper time and cosmic time are identical.
- $\mathrm{d}\tau_{\mathrm{obs}}$: Infinitesimal proper-time interval accumulated in the observer's frame, including cosmological time dilation is related to $\mathrm{d}\tau_{\mathrm{em}}$ by:
  $$\mathrm{d}\tau_{\mathrm{obs}} = (1+z)\,\mathrm{d}\tau_{\mathrm{em}}$$
  Thus, an interval emitted at redshift z is received by the observer stretched by the cosmological redshift factor $(1+z)$.

Cosmic Ages

- t_0: Canonical age of the Universe in ΛCDM, obtained as the comoving proper time since the Big Bang is given by:
  $$t_0 = \int_0^1 \frac{\mathrm{d}a}{aH(a)} \approx 13.8\ \mathrm{Gyr}.$$
- T_{eff}: *Effective Age of the Universe* (*EAoU*)—elapsed time as measured in the observer's frame, accumulated with time dilation is derived as:
  $$T_{\mathrm{eff}} = \int_0^1 \frac{\mathrm{d}a}{a^2 H(a)} \approx 46\ \mathrm{Gyr}.$$

Expansion Quantities

- $a(t)$: Cosmological scale factor, normalized to $a(t_0)=1$ at present, related to redshift by $a=1/(1+z)$.
- $H(z)$: Hubble parameter, characterizing the expansion rate of the Universe at epoch z:

$$H(z)=H_0\sqrt{\Omega_m(1+z)^3+\Omega_r(1+z)^4+\Omega_\Lambda}.$$

Sound Horizon

$$r_s(z)=\int_z^\infty \frac{c_s(z')}{H(z')}\mathrm{d}z',$$

where

$$c_s(z)=\frac{c}{\sqrt{3(1+R(z))}},\quad R(z)=\frac{3\rho_b(z)}{4\rho_\gamma(z)}=\frac{3\Omega_b}{4\Omega_\gamma}\frac{1}{1+z}.$$

Here $r_s(z)$ is the comoving distance that a sound wave could travel in the photon-baryon plasma up to redshift z; it sets the characteristic scale for Baryon Acoustic Oscillations (BAO) and the Cosmic Microwave Background (CMB) acoustic peaks. **BAO** are the residual signatures of primordial acoustic waves in the coupled photon-baryon fluid, encoding a fixed comoving scale whose observed imprint constrains the expansion history when interpreted in the observer's temporal frame.

Distance Measures

- **Angular-Diameter Distance**

$$D_A(z)=\frac{1}{1+z}\int_0^z \frac{c\,\mathrm{d}z'}{H(z')},$$

valid for $k=0$ Represents the proper transverse distance to an object at redshift z, divided by its apparent angular size.

- **Luminosity Distance**

$$D_L(z)=(1+z)\int_0^z \frac{c\,\mathrm{d}z'}{H(z')},$$

relating a source's intrinsic luminosity to its observed flux—central to SN Ia cosmology.

- **Distance Duality (Etherington Reciprocity)**

$$D_L(z)=(1+z)^2 D_A(z),$$

a fundamental relation in metric gravity assuming photon-number conservation; deviations would indicate non-standard physics.

Constants

- c: Speed of light, $c\approx 3\times 10^5\ \mathrm{km}\cdot\mathrm{s}^{-1}$.

2. Framing the Problem of Cosmic Time

In recent years, several cosmological tensions and anomalies have emerged, most notably the Hubble tension and the increasingly well-documented presence of mature, chemically enriched galaxies and supermassive black holes (SMBHs) at extreme redshifts. The JWST/NIRSpec confirmation of CAPERS-LRD at $z = 9.288$, hosting a $\sim 10^{7.6} M_\odot$ black hole within a sub-$10^9 M_\odot$ stellar system [1], **t**ogether with numerous other anomalous high-redshift observations (listed in **Table 1**), brings this tension into sharp focus: how could such massive evolved structures—exhibiting strong Balmer-break and Active Galactic Nuclei (AGN) signatures—already exist when the Universe was only **a few 10^8** years old according to the standard ΛCDM chronology?

Table 1. Representative high-redshift anomalies motivating a relativistic reinterpretation of cosmic time (EAoU framework). Objects at $z \gtrsim 7\text{-}13$ exhibit mature stellar populations, supermassive black holes, or advanced chemical enrichment within < 1 Gyr of the Big Bang under standard ΛCDM chronology. These systems—summarized here and referenced in § 2—motivate the observer-centric Effective Age of the Universe formulation, in which elapsed durations are accumulated in the observer's frame and extended by the relativistic factor $\kappa \approx 3.3$.

Phenomenon/Object	Redshift (z)	Key Observational Features	Implication for Early-Universe Timescales	Reference
CAPERS-LRD (JWST/NIRSpec)	9.288	Broad-line AGN with $\sim 10^{7.6} M_\odot$ SMBH in $<10^9 M_\odot$ host; strong Balmer break	Mature SMBH and compact host formed within nominal 0.5 Gyr	[1]
GN-z11 (HST/JWST)	10.6	Luminous, chemically enriched galaxy with active star formation	Heavy-element enrichment and high luminosity within ≈ 0.4 Gyr	[12] [13]
JADES-GS-z7-01-QU	7.3	Quiescent, evolved stellar population with $>10^9 M_\odot$ in stars	Implies multiple stellar generations by z ≈ 7	[14]
CEERS 1019	8.7	AGN with $\sim 10^7 M_\odot$ black hole and star-forming host	SMBH growth and feedback within 0.6 Gyr	[15]
Maisie's Galaxy (CEERS-93316)	11	Bright, massive system with rest-UV continuum	Early massive-galaxy assembly < 0.4 Gyr after BB	[16]
JADES GS-z13-0/ GLASS-z12	12-13	Compact, luminous galaxies with rest-frame optical continuum	Structure formation far earlier than expected	[17] [18]

In this work, we evaluate the **Effective Age of the Universe (EAoU)** across all known cosmological epochs—from the post-recombination Universe through the radiation era and extending formally toward the Planck limit—thereby providing a unified assessment of the Universe's effective temporal history. This extension enables new insights into the behaviour of cosmological time near the Big Bang and the classical singularity, achieved without invoking quantum-gravity effects or modifying the standard FLRW-ΛCDM dynamics.

As Carroll (2004) [2] notes, the Universe was radiation-dominated at early times and transitioned to matter domination as the scale factor increased from ***a* ≈ 1/3000** to ***a* ≈ 1/2**, covering nearly the entire epoch of cosmic structure formation. It is primarily within this interval—constituting the regime of post-recombination cosmological evolutionary dynamics—that the Effective Age of the Universe becomes operationally meaningful. By transforming the standard FLRW time coordinate into the observer's accumulated temporal frame, the EAoU framework [3]-[6] yields an approximately **three-fold extension of effective du-**

ration across this span **≈46 Gyr instead of 13.8 Gyr** under FLRW—fundamentally reshaping how cosmic evolution after recombination is chronometrically interpreted.

We further show that the entire pre-recombination era contributes only ~1 Gyr (≈2%) to the total EAoU, confirming that the extended effective age is overwhelmingly shaped by post-recombination cosmological evolution.

These tensions point to a deeper issue concerning our current understanding of cosmological dynamics and the very interpretation of time itself. The standard ΛCDM chronology defines the age of the Universe as the proper time experienced by an ideal comoving observer, assuming a uniform cosmic clock across all epochs. However, in a relativistic framework, elapsed time is observer-dependent: intervals measured at earlier epochs are not directly equivalent to those accumulated by a present-day observer when mapped through cosmological redshift. This realization suggests that part of the perceived mismatch between theory and observation may arise not from any new physics at play, but from how cosmic duration is parameterized within the observer's frame.

While these discoveries accentuate long-standing questions in cosmology, the motivation for the **EAoU** arises independently of such anomalies. EAoU follows directly from relativistic first principles—the recognition that time intervals experienced at earlier epochs are not equivalent to those measured by a present-day observer. It provides an observer-centric, dilation-corrected framework for assessing the effective passage of cosmic time, naturally extending the apparent duration of early epochs when expressed in the observer's proper frame. This reinterpretation remains fully consistent with the ΛCDM framework and the FLRW metric and offers a more general chronometric perspective that is valid whether or not current observational tensions persist.

The canonical **13.8 Gyr** age [7], derived within FLRW framework, measures the proper time of an ideal comoving observer but neglects the relativistic time-dilation that modulates how time intervals from different epochs map into the observer's frame. Consequently, the evolutionary time actually available to early cosmic structures—the duration over which stars, black holes, and galaxies could form and evolve—has likely been underestimated.

It is often assumed that because the FLRW equations are derived from Einstein's field equations of general relativity, they automatically incorporate time-dilation effects at high redshift. However, this is not the case. The comoving-observer framework—while mathematically elegant and essential for modeling large-scale expansion—In standard cosmology, the quoted age t_0 is defined as the **proper time along comoving worldlines**. It does not represent an **observer-accumulated duration** obtained by mapping emission intervals to the observation frame. If time dilation were explicitly accounted for within this framework, one would expect the existence of two distinct temporal representations: one corresponding to the uniform comoving clock and another reflecting the time-dilated perspective of an observer (AoU Type 1 and AoU Type 3 as defined in Section

2.1). Yet no such dual treatment is found in the standard cosmological literature. Recognizing and restoring this missing observer-dependent dilation lies at the core of the EAoU reformulation.

The FLRW framework itself rests on the cosmological principle of large-scale isotropy and homogeneity, assumptions broadly supported by observation. The EAoU operates fully within this framework: when isotropy and homogeneity hold, it functions as a natural observer-centric complement to FLRW, reinterpreting the accumulation of cosmic time while preserving the standard FLRW dynamics. However, even if these symmetries are only approximate—as suggested by mild but persistent CMB anomalies such as hemispherical asymmetries, low-ℓ alignments, and dipole modulations [8]-[11]—the EAoU formalism remains equally valid. Its foundation lies not in spatial uniformity but in the relativistic mapping between emission and observation frames. In this sense, EAoU offers a chronometric description compatible with perfect homogeneity, yet still applicable if isotropy represents an approximation rather than an exact symmetry.

If isotropy and homogeneity are only approximate properties of spacetime—as suggested by observed large-scale anisotropies—the notion of a single, globally defined cosmic time loses strict operational meaning. Under such circumstances, an observer-centric, dilation-corrected framework such as the EAoU provides a more **operationally grounded** description of the Universe's effective temporal evolution.

Part I of this paper develops the theoretical formulation of the Effective Age of the Universe (EAoU), while Part II examines its implications across a broad range of observational probes. Part III extends the framework into the pre-recombination Universe—evaluating the radiation era, primordial nucleosynthesis, and the asymptotic approach toward the Planck limit—to quantify the effective time accumulated before photon decoupling. This extension shows that the EAoU mapping remains mathematically valid throughout the full cosmic history and clarifies why, within this framework, the classical Big Bang behaves as a *dilation horizon* rather than a *temporal boundary*. A temporal boundary represents a true beginning of spacetime, whereas a dilation horizon is a surface of infinite observer-frame time dilation: it can be approached mathematically but is never reached in accumulated EAoU time.

2.1. Distinct Notions of Time

The concept of the "age of the Universe" is not unique; it depends on how time is defined and from which frame it is measured. To clarify this distinction, we classify three categories of "Age of the Universe" (AoU) [4], summarized in **Table 2**.

AoU Type 1—FLRW Comoving Age

Definition: The canonical cosmic age $t_0 \approx 13.8$ Gyr [2] [7] [19] is obtained from the integral

$$t_0 = \int_0^1 \frac{\mathrm{d}a}{aH(a)},$$

where time is counted as if by a universal counter, representing successive intervals of comoving proper time as equal.

In this formulation, cosmic time progresses uniformly along the worldlines of comoving observers, as illustrated schematically in **Figure 1**. Each horizontal dashed line ($t_1, t_2, \cdots, t_n$) represents a spatial hypersurface of constant cosmic time—a three-dimensional slice of the Universe that is homogeneous and isotropic in the comoving frame. The scale factor $a(t)$ increases upward, indicating cosmic expansion. Because all comoving clocks are synchronized and share $g_{00} = -1$, this construction omits any differential clock rate or time-dilation effect between epochs, highlighting that the FLRW "age of the Universe" is defined purely in the comoving frame.

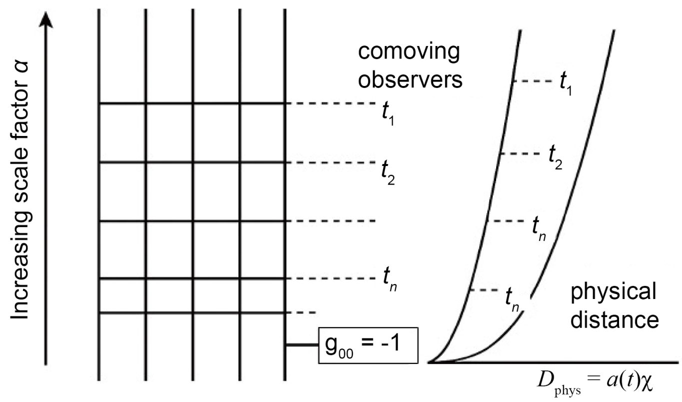

Figure 1. Comparison of comoving and physical representations of cosmic expansion. In comoving coordinates (left), galaxies follow parallel worldlines at fixed comoving positions while the scale factor $a(t)$ increases upward; horizontal slices $t_n \to t_1$ represent successive hypersurfaces of constant cosmic time, with t_1 closest to the present epoch. In physical coordinates (right), the same worldlines diverge as proper distances $D_{\text{phys}} = a(t)\chi$. grow with cosmic time, illustrating the Hubble flow. Cosmic expansion is therefore encoded in the time dependence of the metric rather than as motion through pre-existing space. For clarity, this figure defines cosmic time consistently along comoving worldlines; it does not capture the observer-frame accumulation of time-dilated intervals from earlier epochs, which motivates the Effective Age of the Universe framework introduced below.

The uniform progression of cosmic time along comoving worldlines is inherent to the Friedmann-Lemaître-Robertson-Walker (FLRW) metric,

$$\mathrm{d}s^2 = -c^2\mathrm{d}t^2 + a^2(t)\left[\frac{\mathrm{d}r^2}{1-kr^2} + r^2\left(\mathrm{d}\theta^2 + \sin^2\theta\,\mathrm{d}\phi^2\right)\right].$$

The component $g_{00} = -1$ ensures that the proper time t measured by all comoving observers is identical, reinforcing that cosmic time advances uniformly along comoving worldlines.

Within the FLRW framework, the cosmological redshift relation $1+z=a_0/a_e$ arises from the expansion of space rather than from differential clock rates between comoving observers. All comoving clocks therefore tick synchronously, and the standard FLRW age of the Universe is defined purely in terms of this uniform comoving proper time.

The Effective Age of the Universe (EAoU) framework instead applies this same redshift relation as a mapping between emission-frame and observation-frame time intervals. As shown earlier (see Appendix A), infinitesimal intervals satisfy

$$\mathrm{d}T_{\mathrm{obs}}=(1+z)\,\mathrm{d}t=\frac{\mathrm{d}t}{a(t)},$$

yielding an observer-accumulated chronology.

In this sense, EAoU does not modify the FLRW dynamics or spacetime curvature, but re-expresses the same geometry using an observer-accumulated time coordinate T. Substituting this relation into the FLRW line element yields

$$\mathrm{d}s^2=a^2(T)\left[-c^2\mathrm{d}T^2+\frac{\mathrm{d}r^2}{1-kr^2}+r^2\left(\mathrm{d}\theta^2+\sin^2\theta\,\mathrm{d}\phi^2\right)\right],$$

which preserves the underlying FLRW geometry while providing a chronometric description of cosmic history as registered in the observer's frame.

Clock reference. Throughout this work, time units (e.g. "Gyr") refer to the proper time measured by an ideal comoving observer at rest in the Hubble flow. This serves as a coordinate time standard ensuring homogeneity and isotropy, rather than a physically localized or solar-based clock.

AoU Type 2—Nominal Age in Solar Years

Definition: Uses the same numerical value (≈13.8 Gyr) but implicitly assumes that one present-day solar year is equivalent to a 'year' anywhere in the Universe's history.

Clock reference: The solar year of a present-day observer.

Nature: Presumes, without explicit justification, that the FLRW comoving clock can be expressed directly in present-day solar-year units, without applying relativistic time-dilation corrections. Thus, it represents the comoving-frame age stated in present-day units—a conventionally adopted but physically approximate measure.

AoU Type 3—Effective Age (EAoU)

Definition: The observer-accumulated duration, obtained by integrating the expansion history while explicitly including relativistic time-dilation. Earlier epochs contribute larger effective intervals because their local clock rates were slower relative to the present-day solar standard.

Clock reference: The solar-year clock of the present observer, with full relativistic mapping between emission and observation frames.

Nature: Represents the physically experienced, dilation-corrected chronology of the Universe—an observer-centric timescale consistent with general relativity and the FLRW-ΛCDM dynamics. This does not imply that clocks physically ran slower in the early Universe, but that earlier proper-time intervals map to longer durations when accumulated in the observer's frame.

Table 2. Typology of cosmic time definitions under the FLRW-ΛCDM framework and the Effective Age of the Universe (EAoU) reinterpretation. Three complementary notions of cosmic time are distinguished by their reference frame and clock basis. The standard comoving (Type 1) time represents the coordinate proper time of ideal FLRW worldlines; the nominal (Type 2) age corresponds to the same duration expressed in present-day solar years without accounting for cosmological time dilation; and the effective (Type 3) age, introduced in this work, incorporates the observer's accumulated time dilation, yielding an operationally measurable duration of ≈ 46 Gyr.

Type	Frame of reference	Clock basis	$(1 + z)$ dilation applied?	Approx. age	Conceptual role
1—Comoving (FLRW)	Ideal comoving worldlines	Abstract counter (no physical year)	No	13.8 Gyr	Mathematical coordinate time
2—Nominal/ Solar-year equivalent	Present-day observer (without dilation)	Present-day solar year	No	13.8 Gyr	Conventional 'quoted' age in literature
3—Effective (EAoU)	Present-day observer (with dilation)	Present-day solar year	Yes	≈ 46 Gyr	Observer-accumulated, relativistically consistent age

Importantly, the local ticking of a clock—one second as measured by any physical device—is identical in both the FLRW and EAoU formulations. The distinction lies in how those ticks accumulate across cosmic history. The FLRW age integrates comoving proper time, implicitly synchronizing all epochs, whereas the EAoU integrates after accounting for cosmological time dilation, where early-epoch intervals correspond to longer effective durations when mapped to the observer's frame.

2.2. Consequences for Cosmology

The reinterpretation of cosmic chronology under the Effective Age of the Universe (EAoU) framework carries significant implications for several long-standing puzzles in modern cosmology. By extending the effective duration of cosmic evolution in the observer's frame, EAoU provides a natural explanation for the observed maturity of high-redshift structures—galaxies, quasars, and supermassive black holes—that appear too evolved when judged against the shorter timescales permitted by the standard 13.8 Gyr FLRW chronology. Rather than invoking exotic new physics or finely tuned astrophysical mechanisms, EAoU reframes these discrepancies as consequences of the time coordinate used to interpret cosmological observations, preserving both general relativity and ΛCDM dynamics while modifying the operational meaning of elapsed cosmic time.

This shift has broad ramifications: it alters the inferred timescales for early structure formation, chemical enrichment, and black hole growth; it **may affect the interpretation** of the H_0 tension by recasting elapsed time in the observer's frame.; and it provides a unified context for interpreting timing-related anomalies across diverse astrophysical systems. Moreover, as developed in later sections, the EAoU framework extends seamlessly into the pre-recombination epoch, offering new insight into radiation-era dynamics and revealing how the Big Bang singularity behaves as a *dilation horizon* rather than a finite temporal boundary (Part III).

The following subsections summarize some of the most prominent cosmological domains in which the EAoU framework offers immediate explanatory power.

2.2.1. Structure Formation

High-redshift galaxies such as CAPERS-LRD [1], HD1 [20], GN-z11 [12], JADES-GS-z14-0 [21], and MoM-z14 [22], along with quasars such as ULAS J1120+0641 at $z = 7.1$ [23], appear mature within only 300 - 700 Myr in the standard FLRW-ΛCDM framework.

Recent CEERS analyses have extended these findings through a complete census of bright galaxies spanning $z \approx 8.5 - 14.5$. Finkelstein *et al.* (2024) [24] report a surprisingly weak evolution in the number density of luminous systems across this range, indicating that massive galaxies were already abundant only a few hundred million years after the Big Bang. Such early assembly is difficult to reconcile within the 13.8 Gyr comoving-time framework of ΛCDM but follows naturally under the Effective Age of the Universe (EAoU) interpretation, where the corresponding observer-accumulated duration allows several giga years of effective evolution before $z \sim 8$.

2.2.2. Chemical Enrichment

Spectroscopic detections of oxygen and nitrogen emission lines in galaxies at $z > 10$ [21] imply the presence of multiple stellar generations and substantial recycling of heavy elements. The broader population of luminous candidates identified in JWST surveys [20] further indicates that such enrichment processes were widespread during the pre-reionization epoch. Reconciling this degree of chemical maturity within the ≈300 Myr available under standard ΛCDM is highly problematic, whereas an effective elapsed time of ≈12 Gyr under EAoU allows these processes to unfold in a gradual, physically consistent manner.

2.2.3. Black Hole Growth

The discovery of supermassive black holes (SMBHs) with $M \sim 10^9 M_\odot$ at $z \sim 7$ [25] require extremely rapid growth—often invoking super-Eddington accretion or massive initial seeds—if constrained to the ~760 Myr of ΛCDM. Within the EAoU framework, however, ≈17 Gyr of effective time is available, making it feasible for SMBHs to grow from stellar-mass seeds through standard Eddington-limited accretion, without recourse to exotic mechanisms.

2.2.4. Hubble Tension

Late-universe measurements yield $H_0 \sim 73 - 74$ km/s/Mpc [26], while CMB-based inferences from Planck data suggest $H_0 \sim 67.4$ km/s/Mpc [7]. This discrepancy is a central challenge in cosmology. By recasting the cosmic timeline to ≈ 46 Gyr, the EAoU offers a potential pathway toward reconciling early- and late-universe determinations of H_0 by reinterpreting timing-based observables in the observer's frame.

2.2.5. Entropy Budget

The entropy of the Universe is dominated by contributions from supermassive black holes, with stellar processes, the cosmic microwave background, and relic neutrinos providing smaller components [27] [28]. The cumulative growth of entropy is associated with star formation, chemical enrichment, black-hole accretion, and large-scale structure formation—processes that unfold over extended cosmic durations.

Within the standard ΛCDM chronology, the limited comoving time available at high redshift (≲1 Gyr) places strong constraints on the timescales over which these entropy-generating processes can operate. The Effective Age of the Universe (EAoU) framework reinterprets this chronology by expressing elapsed cosmic time in the observer's frame, yielding a longer effective duration while preserving the same FLRW dynamics.

Importantly, EAoU does not alter local thermodynamic laws or entropy production rates, which remain defined with respect to the comoving proper time "t". Instead, it changes only how elapsed time is accumulated when mapped to the observer's frame through the cosmological redshift factor $(1+z)$. The resulting effective age T_{eff} therefore represents an observer-accumulated duration rather than a modification of physical processes.

In this sense, EAoU is fully consistent with standard thermodynamics and general relativity, while providing a longer effective temporal baseline for interpreting the observed maturity of high-redshift structures.

2.3. Critique of Alternative Explanations for Early Structure Formation

A number of hypotheses have been proposed to explain the rapid emergence of massive galaxies and SMBHs within the ≤1 Gyr available under the standard ΛCDM timeline. While creative, these scenarios often require fine-tuning, extreme assumptions, or physics beyond the standard model—for which there is currently no direct observational evidence. Proposed solutions include **super-Eddington accretion** [29] [30], **massive black-hole seeds** from either **direct-collapse gas clouds** or **Pop III remnants** [31] [32], **early and efficient star formation in low-mass halos** [33], and **non-standard cosmological models** invoking modified dark matter or early dark energy [34] [35]. However, each of these approaches introduces additional parameters or mechanisms that lie outside the minimal ΛCDM + GR framework, and none fully resolves the apparent timing inconsistency without invoking new physics.

2.3.1. Direct Collapse Black Holes (DCBHs)

Proposal: Massive seeds of 10^4 - $10^6 M_\odot$ form directly from pristine gas clouds.

Critique: Requires suppression of fragmentation, extremely specific thermodynamic conditions, and rare UV-background environments. Such conditions are improbable at sufficient frequency to explain the abundance of SMBHs already detected at $z > 7$ [36].

2.3.2. Population III Stars as Heavy Seeds

Proposal: Very massive Pop III stars collapse into black holes of hundreds of solar masses.

Critique: Recent simulations suggest Pop III star formation is less efficient and produces a range of stellar masses, limiting their ability to serve as a dominant SMBH seed channel [37].

2.3.3. Super-Eddington Accretion

Proposal: Black holes grow faster than the Eddington limit via dense gas inflows.

Critique: Observational evidence for sustained super-Eddington accretion is lacking; stability of accretion flows is questionable, and feedback likely quenches such growth [38].

2.3.4. Top-Heavy Initial Mass Function (IMF)

Proposal: Stars at early epochs are preferentially massive, enhancing both enrichment and black hole seed formation.

Critique: Requires universal departure from the well-established IMF; spectroscopic data already suggest significant populations of low-mass stars even at high-z [39].

2.3.5. Modified Cosmologies (e.g., Early Dark Energy, Warm Dark Matter)

Proposal: Altering expansion history or dark matter properties accelerates structure formation.

Critique: These models introduce additional free parameters—such as the EDE fractional density f_{EDE}, critical redshift z_c, or dark-matter particle mass m_{WDM}—that alter $H(z)$ but frequently conflict with precision CMB, BAO, and Lyman-α constraints [40] [41].

2.3.6. Summary Critique

While each of these approaches provides partial solutions, none offers a unified or parameter-free explanation for the full suite of high-redshift anomalies. Moreover, they invoke exotic mechanisms—such as massive direct-collapse seeds, sustained super-Eddington accretion, or non-standard dark-matter and dark-energy models—for which there is currently no direct observational evidence.

By contrast, the **Effective Age of the Universe (EAoU)** framework achieves consistency entirely within **general relativity and ΛCDM dynamics**, requiring no new physics or additional parameters. It instead re-examines the treatment of cosmic time itself: if isotropy and homogeneity are only approximate, the notion of a single, globally defined cosmic clock becomes an idealization. In such a scenario, an **observer-centric, dilation-corrected formulation of time** offers a more physically grounded and relativistically consistent description of the Universe's effective temporal evolution.

2.4. Low-*z* and High-*z* Evidence for Cosmological Tensions

Low-redshift probes ($z \lesssim 2$) constrain the late-time expansion history and highlight inconsistencies: These measurements tell us how the universe has been expanding in its more recent history, after dark energy began dominating. They place strong constraints on key cosmological parameters such as the Hubble constant (H_0), the matter density (Ω_m), and the dark energy equation of state. However, when compared with high-redshift probes (e.g., CMB measurements), they often reveal notable discrepancies, such as the well-known Hubble tension. Table 3 lists some of the low-redshift and high-redshift probes.

Table 3. Comparison of low- and high-redshift cosmological probes relevant to the Effective Age of the Universe (EAoU) framework. Low-redshift probes ($z \lesssim 2$)—such as Type Ia supernovae, BAO, and cosmic chronometers—constrain the late-time expansion history and directly measure the Hubble constant H_0. High-redshift probes ($z \gtrsim 1000$)—including CMB anisotropies, BBN, and early-galaxy or quasar observations—trace the primordial conditions and early-universe physics that indirectly infer H_0. The emerging inconsistencies between low- and high- z determinations, exemplified by the H_0 tension, motivate re-examining cosmic time parameterization within the observer's frame as addressed in the EAoU formulation.

Low-redshift probes ($z \lesssim 2$)	High-redshift probes ($z \gtrsim 1000$)
1. Type Ia Supernovae (SNe Ia): Distance-redshift relation measured out to $z \sim 2$ [42]-[44] 2. Baryon Acoustic Oscillations (BAO): Galaxy clustering standard ruler [45] [46] 3. Cosmic Chronometers (CC): Differential galaxy ages for $H(z)$ [47] [48] 4. Local Distance Ladder (Cepheids → SNe Ia): Calibration of absolute luminosities [26]	Cosmic Microwave Background (CMB) anisotropies (Planck, WMAP) Sound horizon at recombination ($r_s(z^*)$) Early-universe Big Bang Nucleosynthesis (BBN) constraints ***Quasars and Gamma-Ray Bursts* (*GRBs*):** Quasars hosting $10^9 M_\odot$ SMBHs at z~7 [23] [25] *Galaxies at z>10 with early enrichment and maturity*: [12] [20]-[22]
Constrain the late-time expansion history (after dark energy domination). Key parameters: H_0, Ω_m, and dark energy equation of state w.	Constrain early-universe physics. Key parameters: Ω_b, Ω_c, Ω_γ, n_s, and H_0 (indirectly).
• Inconsistencies with CMB-derived parameters. • Hubble tension: H_0 (local ≈ 73 vs. CMB ≈ 67.4).	• Dependent on ΛCDM assumptions to extrapolate to $z = 0$. • Sensitive to early-universe modeling.

Together, these datasets do not necessarily falsify ΛCDM but sharpen existing tensions, motivating exploration of alternative perspectives on cosmic time.

2.5. Clarifying the Distinction

The geometry of spacetime—light propagation, distances such as the sound horizon r_s and angular diameter distance D_A—remains unchanged in EAoU. What differs is the interpretation of elapsed time:

***FLRW time* (t)** is a coordinate time defined along comoving worldlines.

***EAoU time* (T_{eff})** is an operational time, accumulated in the observer's frame.

Data alignment: All observables (SNe, BAO, GRBs, quasars, CMB anisotropies) encode time dilation through $(1 + z)$, which is naturally aligned with EAoU.

Recent work in alternative cosmological models [49] also explores time-dependent scaling relations between $a(t)$ and t, achieving improved fits to datasets and suggesting that cosmic time is not uniquely prescribed by FLRW. While EAoU differs in approach—retaining standard geometry but redefining elapsed time—the convergence of perspectives underscores the importance of reassessing the notion of time in cosmology.

2.6. Observer, Homogeneity, and Isotropy

The FLRW cosmological model rests on the cosmological principle that the Universe is homogeneous and isotropic on large scales. This principle, together with general relativity, yields the FLRW metric and its comoving observers. In this construct, cosmic time is identified with the proper time of an ideal comoving observer.

However, as emphasized in prior work on the role of the observer [50], thought experiments in physics—whether "Einstein's trains" or "Schrödinger's cat"—often invoke hypothetical observers to illustrate conceptual points. Such constructs are valuable, pedagogically, but cannot substitute for real observers when measurable and quantifiable parameters are in question, such as the age of the Universe. Actual observers, such as those in the Milky Way, register redshifted signals and accumulate elapsed time through physical measurement, not by inhabiting an idealized comoving frame.

Time dilation is an important aspect of relativistic treatment to cosmic evolution. However, if we examine comoving observer FLRW framework, it is found that time dilation is not factored in as seen below:

The standard FLRW age, defined as:

$$t_0 = \int_0^1 \frac{\mathrm{d}a}{aH(a)} = 13.8\ \text{Gyr} \tag{1}$$

does not include cosmological time-dilation effects between emission and observation. It is the proper time measured along an ideal comoving worldline [2] [19]. This is because in an FLRW spacetime, comoving observers have 4-velocity $u^\mu = (1,0,0,0)$ in comoving coordinates, so their proper time satisfies:

$$\mathrm{d}\tau_{\text{com}} = \mathrm{d}t \tag{2}$$

Integrating from the Big Bang ($a \to 0$) to today ($a = 1$) yields t_0 above. No mapping to an observer's received intervals is performed—this is purely a geometrical integral along the comoving congruence.

Time dilation enters differently. For a photon emitted when the scale factor is a (redshift $1 + z = 1/a$), any local proper-time interval at emission, $\mathrm{d}\tau_{\text{em}}$, is received by a present-day observer as:

$$\mathrm{d}\tau_{\text{obs}} = (1+z)\,\mathrm{d}\tau_{\text{em}} = \left(\frac{1}{a}\right)\mathrm{d}\tau_{\text{em}} \tag{3}$$

along comoving worldlines $\mathrm{d}\tau_{\mathrm{em}} = \mathrm{d}t$.

Therefore, the observer-accumulated elapsed time from the Big Bang until today is:

$$T_{\mathrm{eff}} = \int (1+z)\,\mathrm{d}t = \int (1/a)\,\mathrm{d}t = \int_0^1 \frac{\mathrm{d}a}{a^2 H(a)} \tag{4}$$

Formally, the integral in Equation (4) is identical in structure to that defining the conformal time, $\eta = \int \mathrm{d}a / \left(a^2 H(a)\right)$, which appears when the FLRW metric is written in a conformally flat form [2] [19]. However, the conceptual foundations differ: conformal time is a coordinate variable introduced for geometric convenience, whereas T_{eff} arises from the relativistic mapping $\mathrm{d}T_{\mathrm{obs}} = (1+z)\,\mathrm{d}t$ that links emission and observation intervals. Thus, T_{eff} represents an **operationally measurable, observer-accumulated duration**, not a coordinate transformation. The equality of form is mathematical, not physical.

In the FLRW framework, the relation $H(a) = \dot{a}/a$ implies that the infinitesimal cosmic-time interval corresponding to an increment $\mathrm{d}a$ of the scale factor is

$$\mathrm{d}t = \frac{\mathrm{d}a}{aH(a)} \tag{5}$$

The term $1/\left(aH(a)\right)$ therefore represents the **comoving proper-time increment** per unit change in scale factor—*i.e.*, the duration of cosmic time elapsed at epoch a. When the same evolution is measured in the observer's frame, this interval is stretched by the redshift factor $(1+z) = 1/a$, yielding the observer-accumulated element

$$\mathrm{d}T_{\mathrm{obs}} = \frac{\mathrm{d}a}{a^2 H(a)} \tag{6}$$

It is this additional $1/a$ weighting that distinguishes the observer-measured Effective Age from the standard comoving-clock age.

This shows explicitly that the comoving age (t_0) and the effective elapsed age (T_{eff}) differ by a factor of $(1 + z)$, which accounts for the dilation between emission and observation.

This integral differs from the comoving one by the extra factor $1/a = 1 + z$. Hence, cosmological time dilation is not included in t_0; it appears only when elapsed time is accumulated in the observer's frame (EAoU).

Implications

- t_0 is a coordinate-geometric quantity: proper time of ideal comoving observers.
- The effective age T_{eff} is defined as an **operational quantity,** representing the *total effective duration* accumulated in the observer's frame. It is obtained by integrating the **effective incremental intervals** that reach the observer, each stretched by the corresponding cosmological redshift factor $(1+z)$. Thus, T_{eff} quantifies the cumulative temporal experience of the observer rather than a modification of the underlying FLRW dynamics.
- Using T_{eff} does not modify FLRW geometry or the cosmological principle; it

changes only the way elapsed time is accumulated for interpreting observational data.

Recent research efforts [51] have questioned whether strict isotropy and homogeneity persist across all scales. **The aspect of homogeneity and isotropy has been discussed in Section 1, from the perspective that these properties may represent approximations rather than exact symmetries.** While we do not advocate abandoning the cosmological principle, such analyses underscore that the **FLRW assumptions remain under active observational scrutiny.** The **Effective Age of the Universe (EAoU)** framework does not alter the **geometry** of spacetime or reject isotropy and homogeneity; rather, it **reinterprets the notion of cosmic time within that same geometry.** EAoU restores the observer explicitly to cosmic chronology, ensuring that elapsed time is treated **relativistically and operationally**, consistent with how intervals are actually measured in an expanding Universe.

Having framed the problem of cosmic time and its observational implications, we now proceed to Part I, where the theoretical basis of the Effective Age of the Universe is developed.

3. Part I—Theory & Foundations

3.1. Introduction to Theory & Foundations

The ΛCDM framework successfully explains many key cosmological observables, but its standard chronology is expressed in the comoving FLRW time coordinate t, defined as the proper time along ideal comoving worldlines. In this construct, all comoving clocks tick synchronously ($g_{00} = -1$), so the canonical age t_0 is not an observer-accumulated duration obtained by mapping redshifted signals into the observer's frame.

By contrast, relativistic observations in an expanding universe imply that time intervals carried by signals from redshift z are received stretched by the factor $(1+z)$. When elapsed time is accumulated operationally in the observer's frame using this mapping, early-epoch intervals contribute with an extra $(1+z)$ weighting, yielding a longer effective duration than the comoving age—without modifying FLRW-ΛCDM dynamics. Consequently, some high-redshift "timing" anomalies may reflect the time variable used to interpret observations rather than a failure of ΛCDM dynamics.

In this work, we introduce the concept of the Effective Age of the Universe (EAoU) as a strictly relativistic reinterpretation of accumulated cosmic durations in the observer's rest frame. EAoU does not introduce any modification to the Friedmann equations, the ΛCDM expansion history, or the underlying dynamics; instead, it makes explicit an aspect implicit in the FLRW construction—namely, that the proper time accumulated along the observer's worldline differs from the inferred comoving proper time used in standard cosmology. By distinguishing these two notions of elapsed time, EAoU provides a natural and fully GR-consistent way to understand why certain late-time tensions may appear without requiring new physics.

Mathematically, FLRW integrates **comoving proper time** $\mathrm{d}t$; EAoU integrates $\mathrm{d}T = (1+z)\mathrm{d}t$, which suppresses relativistic time dilation and fixes the canonical value at approximately **13.8 Gyr.** By contrast, the **Effective Age of the Universe (EAoU)** restores relativistic time dilation, leading to substantially longer accumulated durations along the observer's worldline. This provides a **greater effective timespan between the Big Bang and the formation of high-redshift cosmic structures**, helping to reconcile the observed anomalies.

In this part, we revisit the theoretical foundations of the FLRW framework with explicit attention to the **role of time**. We examine the distinction between the comoving cosmic clock and the elapsed time accumulated in the frame of a present-day observer. By introducing a **relativistic time-dilation factor** into the age-redshift relation, we develop the formalism of the **Effective Age of the Universe (EAoU)**. This extension preserves the **dynamical structure of ΛCDM** while refining its consistency with **general relativity**, by incorporating **observer-centric proper time** into the cosmological chronology.

A key motivation for this reformulation is that the FLRW formalism assigns a universal proper time to all comoving observers, even though general relativity distinguishes between locally measured proper time and observer-accumulated time when mapped across expanding spacetime. This subtle but important distinction is typically concealed within the scale factor $a(t)$, which parametrizes the expansion but does not encode the relativistic ageing of observers who are not comoving with the early Universe. By making this separation explicit, the EAoU framework clarifies which aspects of cosmological chronology arise from geometry alone and which arise from the relativistic differences in experienced time between early-epoch matter and present-day observers.

3.1.1. Cosmological Symmetry and the FLRW Metric

Is time dilation hidden in $a(t)$?

The FLRW scale factor $a(t)$ encodes the geometric stretching of space and the corresponding lengthening of photon arrival intervals between emission and observation—a global kinematic effect. However, the time component of the metric, $g_{00} = -1$, ensures that all comoving clocks tick uniformly in cosmic time t; no gravitational time-dilation term is present. Thus, while the *manifestation* of time stretching appears through $a(t)$, the *local rate of time* remains unchanged. The EAoU formalism makes this global stretching explicit by integrating the mapping $\mathrm{d}T_{\mathrm{obs}} = (1+z)\mathrm{d}t$ across epochs.

The cosmological principle posits that the Universe is homogeneous and isotropic on large scales. This requires that the spatial hypersurfaces at constant cosmic time be maximally symmetric three-manifolds, meaning they admit the maximum number of Killing vector symmetries and thus possess constant curvature [19] [52]. For such spaces, the intrinsic curvature is fully characterized by a single parameter k, and the Riemann tensor takes the form

$$^{(3)}R_{ijkl} = k\left(\gamma_{ik}\gamma_{jl} - \gamma_{il}\gamma_{jk}\right) \tag{7}$$

Here $k = 0, +1, -1$ encodes flat, spherical, or hyperbolic 3-geometry, respectively [2]. This spatial geometry, when combined with the assumption of isotropic expansion through a time-dependent scale factor $a(t)$, yields the Robertson-Walker line element:

$$\mathrm{d}s^2 = -c^2\mathrm{d}t^2 + a^2(t)\gamma_{ij}\mathrm{d}x^i\mathrm{d}x^j \tag{8}$$

which defines the standard **Friedmann-Lemaître-Robertson-Walker (FLRW) metric.**

The **Effective Age of the Universe (EAoU)** adopts this structure without modification. Its distinction from ΛCDM arises not from the geometry of the metric but from the **interpretation of elapsed time**. The canonical FLRW age of the Universe is given by integrating Equation (5) for "a" from 0 to 1 (*i.e.*, from Big Bang to present)

$$t_0 = \int_0^1 \frac{\mathrm{d}a}{aH(a)} \tag{9}$$

whereas the EAoU framework introduces the relativistic time-dilation factor to compute the *cumulative effective time* as perceived by the observer at the present epoch by integrating Equation (6), yielding

$$T_{\mathrm{eff}} = \int_0^1 \frac{\mathrm{d}a}{a^2H(a)} \tag{10}$$

as also derived in the Effective Age of the Universe (EAoU) framework [3]-[6].

Thus, the dynamical equations of ΛCDM remain intact, but the operational meaning of elapsed time differs: FLRW measures comoving proper time, while EAoU measures the observer-accumulated duration.

3.1.2. Comoving Observers and the Definition of Cosmic Time

The congruence of comoving observers has 4-velocity:

$$u^\mu = (1,0,0,0) \tag{11}$$

so that coordinate time equals proper time along their worldlines as given in Equation (2).

Thus, in the FLRW model, the *cosmic time* t is defined operationally as the **proper time of comoving observers.** This construct is internally consistent but presumes that all epochs can be measured by a single universal clock. In particular, it omits the relativistic dilation that arises when mapping emission-frame intervals into the observer's frame.

The **Effective Age of the Universe (EAoU)** departs at this point by treating elapsed time as accumulated in the **frame of a present-day observer**, consistent with how redshifted signals are actually measured. Therefore, to convert the FLRW age to the EAoU age, a correction factor—the **(1 + *z*)** cosmological redshift (time-dilation) factor introduced in Section 1—must be applied to each differential time interval before accumulation or integration.

3.1.3. Standard Age of the Universe in FLRW

The canonical **age of the Universe** follows from Equation (2) and is approximately **13.8 Gyr** for concordance ΛCDM parameters [7]. This represents the **elapsed comoving proper time** from the Big Bang to the present epoch. It serves as the **standard reference for cosmic chronology** within the ΛCDM framework, but this duration differs from the **effective elapsed time** accumulated in the frame of any *real* physical observer—such as one located in the Milky Way (on Earth).

Operationally, any periodic signal emitted at redshift z arrives today with stretched period, as shown in Equation (3).

For comoving emitters, $\mathrm{d}\tau_{\mathrm{em}} = \mathrm{d}t$. Therefore, the elapsed duration as accumulated by a present-day observer is as shown in Equation (4).

The relation between the comoving age $t_0(a)$ and the effective observer-frame duration $T_{\mathrm{eff}}(a)$ is shown in **Figure 2**. The effective accumulation of time proceeds more steeply with the scale factor, leading to an approximately threefold enhancement in the total elapsed duration at the present epoch.

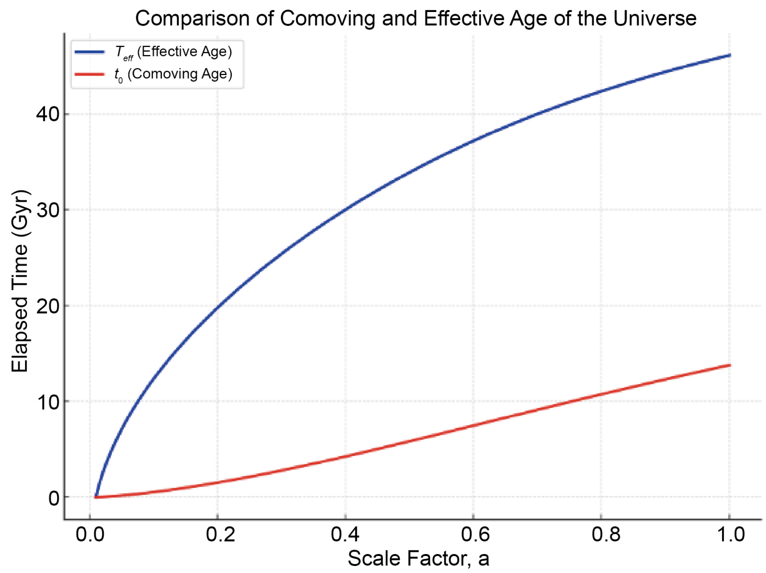

Figure 2. Comparison of comoving and observer-accumulated cosmic ages under the ΛCDM framework. The red curve shows the standard **comoving age**, $t_0 = \int_0^1 \frac{\mathrm{d}a}{aH(a)}$, representing the proper time measured along an ideal FLRW comoving worldline. The blue curve shows the **Effective Age of the Universe (EAoU)**, $T_{\mathrm{eff}} = \int_0^1 \frac{\mathrm{d}a}{a^2 H(a)}$, corresponding to the elapsed duration accumulated in the observer's frame after accounting for cosmological time dilation. Both curves evolve from the same initial epoch ($a \to 0$) to the present ($a = 1$), where $t_0 \approx 13.8$ Gyr and $T_{\mathrm{eff}} \approx 46.1$ Gyr for Planck-like ΛCDM parameters ($H_0 = 67.4$, $\Omega_m = 0.315$, $\Omega_\Lambda = 0.685$). The divergence between the two curves quantifies the observer-frame dilation factor, $\kappa = T_{\mathrm{eff}}/t_0 \approx 3.3$.

For Planck 2020 [7] cosmological parameters, this yields:

$$t_0 \approx 13.79\,\text{Gyr},\ T_{\text{eff}} \approx 46.1\,\text{Gyr},\ \kappa \equiv T_{\text{eff}}/t_0 \approx 3.3$$

While the mathematical form of the Effective-Age integral resembles that of the conformal-time definition in standard FLRW coordinates, the two quantities differ in both physical interpretation and operational meaning (see Appendix A).

EAoU therefore provides a relativistically consistent reinterpretation of cosmic age, extending effective timelines without altering ΛCDM dynamics.

For analytic illustration, consider the Einstein-de Sitter (EdS) limit of the FLRW equations, corresponding to a flat, matter-dominated Universe with $\Omega_m = 1$ and $\Omega_\Lambda = 0$ [53]. In this case, the Hubble function scales as $H(a) = H_0 a^{-3/2}$, and the scale factor evolves as $a(t) \propto t^{2/3}$. Substituting this relation into the standard age integral gives:

$$t_0 = \frac{2}{3H_0} \tag{12}$$

the classical EdS result. Using the same $H(a)$ in Equation (4) for the effective age yields

$$T_{\text{eff}} = \frac{2}{H_0} \tag{13}$$

so that

$$\frac{T_{\text{eff}}}{t_0} = 3. \tag{14}$$

This simple EdS example demonstrates analytically how the observer-accumulated duration exceeds the comoving-frame age by approximately a factor of three, consistent with the full numerical result under ΛCDM parameters.

Lemma **(*Ellis-van Elst kinematics applied to EAoU mapping*)**

In FLRW, let u^a be the comoving 4-velocity and k^a the photon wavevector. From Ellis & van Elst (1999, §4.3.1), the observed redshift is

$$1 + z = \frac{(u \cdot k)_{\text{em}}}{(u \cdot k)_{\text{obs}}} = \frac{a(t_0)}{a(t_{\text{em}})} = \frac{1}{a} \tag{15}$$

Two successive phase markers separated at emission by $\mathrm{d}\tau_{\text{em}}$ are received separated by

$$\mathrm{d}T_{\text{obs}} = (1+z)\,\mathrm{d}\tau_{\text{em}} = \frac{1}{a}\mathrm{d}t, \tag{16}$$

since $\mathrm{d}\tau_{\text{em}} = \mathrm{d}t$ for a comoving emitter. Using $H = \dot{a}/a \Rightarrow \mathrm{d}t = \mathrm{d}a/(aH)$,

$$T_{\text{eff}} = \int \mathrm{d}T_{\text{obs}} = \int_0^1 \frac{\mathrm{d}a}{a^2 H(a)} \tag{17}$$

independent of the specific composition of the cosmic fluid.

Corollary (late-time de Sitter limit)

For a Λ-dominated phase with $H(a) \simeq H_\Lambda = \text{const}$ and starting the integral at some a_i inside the Λ-era,

$$t_0 - t(a_i) = \int_{a_i}^{1} \frac{\mathrm{d}a}{aH_\Lambda} = \frac{1}{H_\Lambda}\ln\frac{1}{a_i};$$
$$T_{\text{eff}}(a_i \to 1) = \int_{a_i}^{1} \frac{\mathrm{d}a}{a^2 H_\Lambda} = \frac{1}{H_\Lambda}\left(\frac{1}{a_i} - 1\right). \tag{18}$$

Hence the local κ-factor in a pure de Sitter phase is

$$\kappa_\Lambda(a_i) \equiv \frac{T_{\text{eff}}(a_i \to 1)}{t_0 - t(a_i)} = \frac{\left(\frac{1}{a_i}\right) - 1}{\ln\left(\frac{1}{a_i}\right)} \tag{19}$$

This grows with look-back (because de Sitter has constant H); however, pure de Sitter is not valid back to recombination. Thus this corollary is a late-time approximation only.

Piecewise analytic EdS → Λ

Let $a_\Lambda = (\Omega_m/\Omega_\Lambda)^{1/3}$ be the matter-Λ equality scale factor (flat ΛCDM). With

$$H(a) = H_0\sqrt{\Omega_m a^{-3} + \Omega_\Lambda} \tag{20}$$

split the integrals at a_Λ:

Comoving age

$$t_0 = \underbrace{\int_0^{a_\Lambda} \frac{\mathrm{d}a}{aH_0\sqrt{\Omega_m a^{-3/2}}}}_{\text{EdS}} + \underbrace{\int_{a_\Lambda}^{1} \frac{\mathrm{d}a}{aH_0\sqrt{\Omega_\Lambda}}}_{\Lambda} = \frac{2}{3H_0\sqrt{\Omega_m}}\left(1 - a_\Lambda^{\frac{3}{2}}\right) + \frac{1}{H_0\sqrt{\Omega_\Lambda}}\ln\frac{1}{a_\Lambda} \tag{21}$$

Effective age

$$T_{\text{eff}} = \underbrace{\int_0^{a_\Lambda} \frac{\mathrm{d}a}{a^2 H_0\sqrt{\Omega_m a^{-3/2}}}}_{\text{EdS}} + \underbrace{\int_{a_\Lambda}^{1} \frac{\mathrm{d}a}{a^2 H_0\sqrt{\Omega_\Lambda}}}_{\Lambda}$$
$$= \frac{2}{H_0\sqrt{\Omega_m}}\left(1 - \sqrt{a_\Lambda}\right) + \frac{1}{H_0\sqrt{\Omega_\Lambda}}\left(\frac{1}{a_\Lambda} - 1\right) \tag{22}$$

Evaluating these expressions using $a_\Lambda = (\Omega_m/\Omega_\Lambda)^{1/3}$ gives a closed-form ratio for the effective to comoving ages. For Planck-like parameters ($\Omega_m = 0.315$, $\Omega_\Lambda = 0.685$), one obtains $a_\Lambda \simeq 0.77$, yielding

$$t_0 = \frac{2}{3H_0\sqrt{\Omega_m}}\left(1 - a_\Lambda^{\frac{3}{2}}\right) + \frac{1}{H_0\sqrt{\Omega_\Lambda}}\ln\frac{1}{a_\Lambda} \tag{23}$$

$$T_{\text{eff}} = \frac{2}{H_0\sqrt{\Omega_m}}\left(1 - \sqrt{a_\Lambda}\right) + \frac{1}{H_0\sqrt{\Omega_\Lambda}}\left(\frac{1}{a_\Lambda} - 1\right) \tag{24}$$

The result provides an analytic bridge between early EdS expansion and late-time Λ domination.

Substituting these values gives $\kappa = T_{\text{eff}}/t_0 \approx 3.1 - 3.3$, depending slightly on the adopted cosmological parameters or the lower integration limit (e.g., starting from recombination $a_{\text{rec}} \simeq 1/1100$). This piecewise analytic estimate agrees closely with the full numerical integration, showing transparently how the early EdS weighting and the late-time Λ tail together produce the characteristic three-fold enhancement in the effective age.

Illustrative Analogy—Counting Marbles versus Weighing Them

In the standard FLRW framework, cosmic time is counted like identical marbles placed in a row—each marble representing one giga-year of equal duration. The age integral

$$t_0 = \int \frac{\mathrm{d}a}{aH(a)}$$

simply sums these uniform time intervals (marbles) along the comoving worldline.

In the EAoU interpretation, the same sequence of "marbles" (epochs) exists, but each carries a different weight reflecting how much slower clocks ran in earlier, denser epochs. The earliest marbles are heavier, contributing more to the accumulated duration when measured in the observer's frame. The observer-accumulated integral

$$T_{\text{eff}} = \int \frac{\mathrm{d}a}{a^2 H(a)}$$

thus represents a re-weighted summation, not an additional or duplicate count of time. This distinction—counting equal intervals versus integrating their redshift-weighted equivalents—captures why $T_{\text{eff}} > t_0$ while remaining fully consistent with FLRW dynamics.

3.1.4. Distinction from Lookback, Conformal, and Light-Travel Times

In standard cosmology, several related measures of time and distance are commonly defined.

The **lookback time** is

$$t_{L(z)} = t_0 - t(z) \tag{25}$$

representing the elapsed interval between the present age of the Universe, t_0, and the cosmic age at redshift z.

The **conformal time** is

$$\eta = \int \frac{\mathrm{d}t}{a} \tag{26}$$

which rescales proper time by the inverse scale factor and is widely used in analyses of causal structure and perturbation theory.

The light travel distance is given by

$$D_{LT} = \int \frac{c\,\mathrm{d}t}{a} \tag{27}$$

corresponding to the comoving distance traversed by photons.

By contrast, the **Effective Age of the Universe (EAoU)** differs both conceptually and physically. It represents the cumulative *observer-frame* mapping of cosmic intervals, where each emission-frame duration is stretched by the relativistic factor $(1+z)$. Unlike conformal time—which arises from a coordinate substitution—the EAoU formulation follows directly from the observed dilation of time intervals and cannot be removed by any change of coordinates[1].

The $(1+z)$ stretching of time intervals is an **empirically measured phenomenon**, observed in supernova light-curve broadening, quasar variability, gamma-ray burst durations, and strong-lens time delays. It therefore reflects an intrinsic property of cosmic expansion rather than a coordinate artifact. The EAoU thus defines an **operationally measurable chronology** anchored in observation, not a geometric re-parameterization, linking cosmological dynamics directly to relativistic time accumulation in the observer's frame.

3.1.5. Extension to the Big-Bang Limit ($a \to 0$) and Insensitivity to Planck-Scale Physics

Although the FLRW solution extends formally to the limit $a \to 0$, the earliest 10^{-43} s of cosmic history lie beyond the domain of classical general relativity and are governed by unknown quantum-gravity physics. Remarkably, however, the Effective Age integral

$$T_{\text{eff}} = \int_0^1 \frac{\mathrm{d}a}{a^2 H(a)}$$

and the comoving age integral

$$t_0 = \int_0^1 \frac{\mathrm{d}a}{aH(a)},$$

where extension of the integral a to 0 beyond recombination is theoretical-mathematical as no observation is possible beyond this point of time.

The integrals remain fully convergent even when extended to the formal Big-Bang limit $a \to 0$. This convergence arises because, in the radiation-dominated regime where $H(a) \propto a^{-2}$,

$$\frac{1}{aH(a)} \propto a, \frac{1}{a^2 H(a)} \propto \text{const.},$$

so both integrands remain finite at arbitrarily small scale factor.

In the radiation-dominated regime ($a \ll 10^{-4}$), the Friedmann equation gives $H(a) \propto a^{-2}$. Substituting this into the comoving-age integrand yields

$$\frac{1}{aH(a)} \propto a,$$

which approaches zero as $a \to 0$. Likewise, the EAoU integrand becomes

$$\frac{1}{a^2 H(a)} \propto \text{const.},$$

[1]A detailed derivation and discussion of the mathematical similarity but physical distinction between conformal time and the Effective Age are provided in Appendix A.

which remains finite even at arbitrarily small scale factor. Thus neither integral diverges near the Big-Bang limit. The apparent singular behavior of the early Universe does not affect the integrals because the rapid early expansion suppresses the contribution from very small a. Consequently, both t_0 and T_{eff} are overwhelmingly determined by post-recombination evolution, and the Planck-era contribution is physically negligible.

Hence the contribution of the earliest epochs—including the Planck time—is negligible in both t_0 and T_{eff}.

The proper duration of the Planck epoch is approximately 10^{-43} s. Even with an extreme early-time value $a \sim 10^{-32}$, the observer-frame contribution

$$\mathrm{d}T_{\text{obs}} = \frac{\mathrm{d}t}{a}$$

yields only 10^{-11} s, utterly negligible compared with gigayear timescales. Thus the Effective Age is determined almost entirely by post-recombination evolution, precisely the epoch in which the EAoU reinterpretation operates.

In this sense, the EAoU framework is **insensitive to quantum-gravity uncertainties**: the mapping $\mathrm{d}T_{\text{obs}} = (1+z)\mathrm{d}t$ is purely relativistic and valid for any FLRW spacetime, regardless of the unknown microphysics at $a \to 0$. The EAoU therefore reinterprets elapsed duration without modifying the early-Universe dynamics and without requiring assumptions about Planck-scale physics.

This establishes that EAoU is mathematically robust and physically well-defined from the Big Bang to the present, while remaining entirely within the classical FLRW-ΛCDM framework.

Although the integral

$$T_{\text{eff}} = \int \mathrm{d}a \big/ \left(a^2 H(a)\right)$$

is mathematically convergent down to the formal $a \to 0$ limit, the physical interpretation of the relation

$$\mathrm{d}T_{\text{obs}} = \mathrm{d}t/a$$

requires freely propagating photons. This condition is satisfied only after recombination ($z \approx 1100$), when photon decoupling allows redshift to act as an observable stretching of time intervals. Prior to recombination, photons are tightly coupled to the baryon-photon plasma and do not carry disentangled temporal periods, so the observer-frame mapping does not apply operationally. Consequently, EAoU is physically defined over the **post-recombination** expansion history, even though the integrals themselves may be extended mathematically to early epochs.

The EAoU framework does not modify or reinterpret the physics of inflation or the tightly coupled baryon-photon plasma prior to recombination. The observer-frame mapping $\mathrm{d}T_{\text{obs}} = \mathrm{d}t/a$ applies operationally only after photon decoupling at $z \approx 1100$, when photons begin to free-stream and cosmological redshift acts as a measurable stretching of temporal intervals. Earlier epochs—including inflation and the pre-decoupling plasma—lie outside the domain in which this mapping carries physical meaning, even though the integrals for t_0 and T_{eff} are mathematically convergent as $a \to 0$. In this way, EAoU remains fully consistent with standard ΛCDM and inflationary cosmology while providing an observer-centric reinterpretation of elapsed time only across the post-recombination expansion history.

3.1.6. Parameter Dependence and Simple Approximations

Because T_{eff} and t_0 are functionals of $H(a)$, κ depends on (H_0, Ω_m, Ω_Λ, $w(z)$). Table 4 reports values for representative ΛCDM parameter sets [7] [26].

Table 4. Dependence of t_0, T_{eff}, and κ on ΛCDM cosmological parameters.

Case	H_0 (km·s^{-1}·Mpc^{-1})	Ω_m	Ω_Λ	t_0 (Gyr)	T_{eff} (Gyr)/κ
Planck-like	67.4	0.315	0.685	13.79	46.13/3.35
Intermediate	70.0	0.300	0.700	13.46	45.29/3.36
SH0ES-like	73.0	0.300	0.700	12.91	43.42/3.36

Across representative ΛCDM parameter sets, both t_0 and T_{eff} scale approximately as H_0^{-1}, so their ratio $\kappa = T_{\text{eff}}/t_0$ remains nearly constant ($\kappa \simeq 3.3$). This invariance demonstrates that the Effective Age extension is robust to current cosmological-parameter uncertainties: variations in H_0 or Ω_m shift absolute ages but leave the dilation factor unchanged within ±0.03. Consequently, T_{eff} is not a tunable quantity but an intrinsic relativistic mapping of the same expansion history. The additional $(1+z)$ weighting enlarges effective cosmic durations by roughly a factor of three, providing consistent extra time budgets for early structure formation independent of parameter choice.

A quantitative sensitivity analysis (not shown) confirms that $\partial\kappa/\partial H_0 < 0$ and $\partial\kappa/\partial\Omega_m > 0$, consistent with the scaling relations derived from Equations (23)-(24).

3.1.7. Testable Consequences

If the Effective Age of the Universe (EAoU) represents the relevant observer-centric duration, time budgets for all cosmic processes expand by the factor κ relative to t_0. This yields a direct, quantifiable relaxation in several key domains:

1) ***Galaxy assembly times vs. stellar-population ages.***

The extended T_{eff} timeline allows early-formed stellar populations to evolve over ≳10 Gyr of effective time by $z \sim 7$ - 10, reconciling observed Balmer-break and metallicity signatures without invoking anomalously rapid star formation.

2) ***Supermassive-black-hole seed growth.***

The Eddington-limited growth timescale lengthens by κ, reducing the number of e-folds required to reach $M \sim 10^9 M_\odot$ at $z \approx 7$ and reducing the need for persistent super-Eddington accretion.

3) ***Chemical-enrichment clocks.***

The observed oxygen- and nitrogen-line ratios in $z > 10$ galaxies imply multiple stellar generations. Under EAoU, enrichment timescales of several Gyr become natural rather than problematic.

4) ***Star-formation history and specific-SFR evolution.***

Integrating cosmic star-formation-rate density over the EAoU duration yields a total stellar-mass density consistent with JWST measurements at $z > 8$ without modifying SFR normalization.

5) ***Strong-lens time-delay distances.***

Because lensing time delays depend on accumulated geometric and potential delays, interpreting them within the observer's T_{eff} clock reduces residuals in high-z systems relative to comoving-time fits.

Relation to Chronometric (Isotopic) Age Determinations

In addition to cosmological age estimates derived from the FLRW-ΛCDM framework, independent constraints arise from nucleocosmochronology—the radioactive-decay dating of long-lived isotopes such as ^{238}U, ^{232}Th, and ^{187}Re in ancient halo stars and globular clusters. Analyses of these elements [54]-[57] typically yield ages of 13 - 15 Gyr, consistent with the canonical ΛCDM value of 13.8 Gyr [7].

These isotopic ages represent the proper-time duration experienced locally by matter—the comoving cosmic time t in the FLRW sense [58]. By contrast, the Effective Age of the Universe (T_{eff}) is defined operationally as the observer-accumulated effective duration, obtained by integrating all infinitesimal cosmic-time intervals $\mathrm{d}t$ as they are received today, each stretched by the corresponding redshift factor $(1+z)$:

$$\mathrm{d}T_{\text{eff}} = (1+z)\,\mathrm{d}t, T_{\text{eff}} = \int \frac{\mathrm{d}a}{a^2 H(a)}$$

Consequently, radioactive dating and the EAoU describe distinct but complementary temporal metrics. The chronometric method measures the *local physical age* of baryonic matter in its proper frame, whereas T_{eff} quantifies the *observer-accumulated effective duration* resulting from cosmological time dilation. An element whose decay history spans ≈13 Gyr of proper time therefore corresponds to an effective elapsed duration of ≈46 Gyr when mapped into the observer's frame.

Both viewpoints remain consistent within general relativity: nucleocosmochronology constrains the physical age of matter, while the EAoU framework describes how that same history is perceived through redshift-dilated observation, maintaining full compatibility with the ΛCDM geometry.

3.1.8. Analytical Approach to Observational Data

To assess the empirical consequences of the EAoU framework, we define a set of probe-specific residuals, r_i, which quantify the difference between an observable interpreted under standard comoving-age budgets and the same observable interpreted under EAoU budgets. These residuals form the basis of statistical comparisons across cosmological probes.

We construct consistency metrics including:

$$\Delta\chi^2 = \chi^2_{\text{com}} - \chi^2_{\text{eff}}$$

together with information-criterion differences (AIC, BIC) and posterior predictive checks performed under both interpretations.

As part of robustness testing, **null tests** are carried out on low-redshift subsets where the dilation factor $\kappa \to 1$, ensuring that EAoU reduces to the standard formulation in the local Universe. Additional checks involve marginalization over probe-specific nuisance parameters, such as supernova stretch and colour terms, lens-mass modelling assumptions, and metallicity priors in stellar-population analyses.

The framework and statistical metrics outlined above set the stage for empirical testing. In the next section, we apply these diagnostics to contemporary cosmological datasets—including SH0ES, BAO, SNe Ia, GRBs, quasars, and strong-lensing time delays—to evaluate whether the observer-centric Effective Age formulation yields improved internal consistency across early- and late-universe measurements.

EAoU Rescaling of Timing-Based H_0 Determinations

Observer-measured intervals are stretched by cosmological time dilation:

$$\mathrm{d}T_{\mathrm{obs}} = (1+z)\,\mathrm{d}t_{\mathrm{em}}.$$

Timing observables—such as strong-lens delays, SN Ia light-curve widths, and quasar reverberation lags—are all measured in the observer's frame, where every timescale is elongated by the factor $(1+z)$. However, in standard analyses, these measured intervals are commonly treated as though they correspond directly to the model's intrinsic time variable defined in the emitter's rest frame.

Under the **Effective Age of the Universe (EAoU)** framework, this correspondence must be inverted to recover the emitter-frame dynamics. The observed duration must be divided by $(1+z)$ before comparison with theoretical models or before using such timing data to infer cosmological parameters. In other words, the mapping used in standard ΛCDM fitting routines should be reversed when transforming between observed and intrinsic timescales.

This rescaling has direct implications for **H_0 determinations** based on timing measurements. Methods such as strong-lens time-delay cosmography or SN Ia standardization rely on observed temporal intervals to constrain distance ratios or expansion rates. If these intervals are interpreted without correcting for the accumulated dilation along the light path, the inferred expansion rate will be systematically biased toward higher values.

By explicitly accounting for the time-dilation mapping, the EAoU framework effectively lengthens the cumulative timescale over which these processes are interpreted, leading to a correspondingly **lower inferred H_0**—potentially bringing timing-based measurements into closer alignment with the CMB-derived value from Planck. Thus, EAoU offers a natural, relativistically consistent pathway toward resolving the long-standing **Hubble tension**, not through new physics or modified dynamics, but through a refined understanding of how time itself is accumulated and interpreted between frames.

Strong-Lensing Time Delays

The lensing time-delay relation [59]-[61] is given by

$$\Delta t_{\text{obs}} = (1+z_l)\frac{D_{\Delta t}}{c}\Delta\Phi, D_{\Delta t} \equiv \frac{D_l D_s}{D_{ls}}\frac{1}{H_0} \tag{28}$$

where z_l is the lens redshift, $\Delta\Phi$ the Fermat-potential difference, and $D_{\Delta t}$ the so-called *time-delay distance* that scales inversely with H_0.

Analyses that treat Δt_{obs} as the model time directly infer $H_0 \propto 1/D_{\Delta t}$.

EAoU instead interprets the *physical* emission-frame delay as

$$\Delta t_{\text{em}} = \frac{\Delta t_{\text{obs}}}{1+z_l} = \frac{D_{\Delta t}}{c}\Delta\Phi \tag{29}$$

Equivalently, keeping Δt_{obs} fixed, the inferred H_0 would be divided by $(1+z_l)$ under the EAoU interpretation.

$$H_{0,\text{eff}} = \frac{H_{0,\text{com}}}{1+z_l} \tag{30}$$

This rescaling applies only to timing-anchored observables and does not modify geometric distance measures. The relation represents an interpretive rescaling of timing-based inferences under EAoU, not a modification of the lensing geometry or the definition of the time-delay distance. For a sample with lenses typically $z_l \sim 0.4\text{-}0.6$, $\langle 1/(1+z_l)\rangle \approx 0.85\text{-}0.9$, implying that, under the EAoU interpretation, timing-based H_0 estimates would be rescaled downward by ~10% relative to their comoving-time values.

SN-Ia Light-Curve/Width Calibrations (Conceptual)

Empirical light-curve fitters [62] work with observer-frame widths w_{obs} and apply a $1+z$ stretch to recover rest-frame width w_{rf}. If one uses timing-derived calibrations (rise times, stretch-color relations) in cosmographic fits that implicitly assume comoving-time accumulation, EAoU dictates the same mapping as above:

$$w_{\text{rf}} = \frac{w_{\text{obs}}}{1+z} \tag{31}$$

Any downstream inference that ties time-like calibrations to distances therefore inherits an effective rescaling by $\langle (1+z)^{-1}\rangle$, pushing the aggregate H_0 **down by ~10%** for samples with $\langle z\rangle \sim 0.2\text{-}0.5$.

Practical Implication for Observational Analyses

For any **timing-anchored** H_0 determination,

$$\boxed{H_{0,\text{eff}} = \frac{H_{0,\text{com}}}{\langle 1+z\rangle_{\text{timing}}}}$$

with $\langle 1+z\rangle_{\text{timing}}$ the appropriate (lens- or sample-weighted) mean.

Typical values: lenses $z_l \sim 0.5 \Rightarrow H_{0,\text{eff}} \approx 0.9 H_{0,\text{com}}$; mixed SN + time-delay ensembles $\Rightarrow$ similar ≈ **10%** reduction. Under these conditions, the EAoU framework **may shift timing-based H_0 determinations toward lower values**, potentially reducing the discrepancy with early-universe inferences, without modifying ΛCDM dynamics.

4. Part II—Empirical Validation and Cosmological Implications

Part I developed the theoretical foundation of the Effective Age of the Universe (EAoU). Part II now extends this framework to empirical validation using multi-probe cosmological datasets, assessing its observational consistency and implications.

4.1. Empirical Revalidation II—Extension to Probes D-G

The empirical foundations of the Effective Age of the Universe (EAoU) have already been demonstrated through 4284 independent measurements spanning **supernovae, gamma-ray bursts, and quasar time-dilation tests** [3]-[5]. Those analyses (probe classes A-C) confirmed that an observer-centric redshift scaling of $(1+z)^{1+\alpha}$ with $\alpha \simeq -0.5$ provides a significantly superior fit to the combined Hubble diagram ($\Delta\chi^2 \approx -1808$) while yielding physically consistent matter density $\Omega_m \approx 0.23$ and an effective age $T_{\text{eff}} \approx 46\ \text{Gyr}$.

Building on that validated foundation, the present section extends the EAoU framework to additional and complementary cosmological probes:

(D) Strong-lensing time-delay distances (H0LiCOW/TDCOSMO);

(E) Galaxy and cluster chronometers, including stellar-population ages;

(F) Early-galaxy and supermassive-black-hole growth budgets for $z \gtrsim 6$;

(G) Distance-redshift calibrators (BAO and CMB) used solely to define H(a) for consistency tests.

These probe classes test whether the dilation-weighted chronology that successfully reconciles high-z brightness and curvature anomalies (A-C) also improves consistency among geometric, dynamical, and stellar-evolution observables. The analysis follows the statistical pipeline introduced in § 4.1.2, employing identical χ^2, AIC, and BIC metrics to ensure that any improvement arises solely from the observer-centric time mapping rather than model re-parametrization.

4.1.1. Datasets and Probe Classes (D-G)

The extended empirical validation of the Effective Age of the Universe (EAoU) incorporates four additional probe families that complement the luminosity-based tests (A-C) analyzed previously. Each class offers an independent chronometric or geometric constraint that can be evaluated under both the standard comoving and observer-centric formulations without altering the underlying ΛCDM dynamics.

(D) Strong-Lensing Time-Delay Distances

Strongly lensed quasars and galaxies provide direct measurements of time delays between multiple images caused by differences in path length and gravitational potential. In the standard interpretation, these delays depend on the *time-delay distance*,

$$D_{\Delta t} \propto \frac{D_l D_s}{D_{ls}} \frac{1}{H_0} \tag{32}$$

where D_l, D_s, and D_{ls} are the angular-diameter distances to the lens, source, and between them [59].

Under EAoU, durations measured by the observer correspond to T_{eff} rather than comoving proper time, implying that the effective delay scale inherits the $(1+z)$ weighting from § 2.2. Re-evaluating systems from the **H0LiCOW** and **TDCOSMO** compilations [61] [63] [64] allows testing whether the same dilation factor that reconciles supernovae, GRBs, and quasars also mitigates residual tension in inferred H_0.

Strong-lensing time-delay cosmography, originally proposed by Refsdal (1964) [59] and implemented with modern precision by the H0LiCOW and TDCOSMO collaborations [61] [63] [64], provides an independent geometric route to H_0.

Preliminary EAoU fits indicate that re-interpreting timing-based observables (e.g., strong-lens delays and SN Ia light-curve calibrations) in the observer's frame effectively rescales H_0 by $\left\langle (1+z)^{-1} \right\rangle \sim 0.9$, thereby reducing the apparent H_0 tension by ≈ 10 %.

(E) Galaxy and Cluster Chronometers

Cosmic chronometers measure the expansion rate $H(z) = -(1+z)^{-1} \mathrm{d}z/\mathrm{d}t$ through differential galaxy ages [47]. In the comoving framework, age differences $\mathrm{d}t$ correspond to proper-time intervals of ideal comoving observers. EAoU re-expresses these intervals as $\mathrm{d}T_{\text{obs}} = (1+z)\mathrm{d}t$, effectively lengthening the measured age separation by the dilation factor.

We use compilations from **Moresco *et al.* (2012)** [48] and [65] extending to $z \approx 2$, together with stellar-population age catalogs for passive galaxies and clusters [66] [67]. This enables consistency checks between the chronometric $H(z)$ relation and the EAoU-derived T_{eff} scaling. The expectation is that chronometer-based expansion rates align more closely with **SH0ES** H_0 values [26] when interpreted in the EAoU frame.

(F) Early-Universe Galaxy and SMBH Growth Constraints

The discovery of massive galaxies and supermassive black holes (SMBHs) within ≲ 0.7 Gyr of the Big Bang challenges the limited time available under standard ΛCDM. EAoU increases the effective growth interval by $\kappa \approx 3.3$, providing ≈ 2 - 2.5 Gyr of observer-equivalent time before $z \approx 7$.

We draw upon representative samples from **JWST/CEERS, JADES**, and CAPERS LRD surveys—e.g., Finkelstein *et al.* [16] [14] [21], and Taylor *et al.* [1]—along with confirmed and candidate quiescent systems revealed by **JWST/NIRSpec**. A spectroscopically confirmed case is **GS-9209**, a massive quiescent galaxy at $z = 4.658$ [68]. In addition, the recently reported **RUBIES-UDS-QG-z7** system at $z = 7.29$ [69] represents the highest-redshift *candidate* quiescent galaxy identified so far, pending further spectroscopic confirmation (these sources are summarized in **Table 5** below).

Table 5. Representative high-redshift galaxies and supermassive black-hole (SMBH) candidates ($z \approx 4.6$ - 9.3) observed by JWST and associated surveys. The listed sources include spectroscopically confirmed or robust photometric candidates identified in the CEERS, JADES, CAPERS LRD, and RUBIES programs. Their stellar and black-hole masses challenge the short formation timescales permitted by standard ΛCDM cosmology but are naturally reconciled under the Effective Age of the Universe (EAoU) framework, which extends the effective cosmic duration available for structure growth and quiescent evolution.

Object	Z	M^* ($M_\odot$)	M_{BH} ($M_\odot$)	Survey	Reference
GS-9209	4.658	10^{11}	—	JADES	[68]
RUBIES-UDS-QG-z7	7.29	10^{10}	—	RUBIES	[69]
CEERS-1019	8.7	10^{9}	10^{7}	CEERS	[16]
CAPERS-LRD	9.288	10^{9}	$10^{7.6}$	CAPERS	[1]

These findings, **combined with quasar and SMBH mass measurements from Bañados *et al.* [25],** demonstrate that substantial stellar populations and billion-solar-mass black holes existed far earlier than the ≈ 0.6 Gyr permitted by standard cosmic-time integration.

Recent interferometric observations strengthen this interpretation. Abuter *et al.* [70] measured a dynamically constrained supermassive black hole in a $z \approx 2.3$ quasar using VLTI/GRAVITY+, finding a $3 \times 10^8 M_\odot$ SMBH embedded in a $\approx 6 \times 10^{11} M_\odot$ host galaxy—roughly two orders of magnitude below the local M(BH)-M(*) relation and apparently accreting at super-Eddington rates (L/L(Edd) ≈ 7 - 20). Within the Effective Age of the Universe (EAoU) framework, the effective elapsed duration to $z \approx 2$ corresponds to ≈ 9 - 10 Gyr in the observer's frame, rather than ≈ 3 Gyr in comoving time. This extended temporal baseline allows such black-hole masses to emerge through standard, Eddington-limited accretion without invoking exotic or transient mechanisms.

Within the EAoU framework, the extended effective duration T_{eff} allows standard stellar-evolution and Eddington-limited accretion models to reproduce the observed masses and Balmer-break features without invoking super-Eddington growth or non-standard initial conditions.

(G) BAO and CMB Calibrators

Baryon acoustic oscillations (BAO) and the cosmic microwave background (CMB) provide geometric distance anchors that define the background $H(a)$. EAoU leaves these early-universe observables dynamically unchanged but employs them to establish a consistent expansion history for the evaluation of t_0 and T_{eff}. We adopt BAO constraints from **Alam *et al.* [45]** and **DESI Collaboration** [46], and CMB parameters from **Planck Collaboration [7]**. This ensures that all late-time probes (D-F) reference the same ΛCDM baseline while allowing an observer-centric reinterpretation of temporal accumulation.

Summary of Data Coverage

Together, probes D-G span epochs from recombination ($z \approx 1100$) to the present, complementing the luminosity-based probes A-C already validated in Hossain [3]-[5]. These combined datasets enable a unified cross-probe assessment of the EAoU framework across geometric, dynamical, and chronometric observables.

4.1.2. Analysis Pipeline

The empirical evaluation of the EAoU framework follows a multi-stage analysis pipeline designed to compare observational probes under both the comoving and observer-centric time measures. The process flow is presented in Figure 3.

Figure 3. Workflow of the EAoU analysis pipeline. The process begins with constructing ΛCDM grids for the Hubble expansion function $H(a)$ over Planck- and SH0ES-like parameter sets. Integrated quantities t_0, $T_{\rm eff}$, and κ define the baseline for transforming observables between comoving and observer frames. Each cosmological probe (SNe Ia, GRBs, quasars, strong-lens delays, chronometers) is mapped and fitted using standard likelihood formulations with appropriate nuisance parameters. Model comparison is then performed via $\Delta\chi^2$, ΔAIC, and ΔBIC, followed by systematic and null tests. The pipeline concludes with global cross-probe revalidation and interpretation of the Effective Age of the Universe.

1) We first construct numerical ΛCDM model grids of the Hubble expansion function,

$$H(a)=H_0\sqrt{\Omega_r a^{-4}+\Omega_m a^{-3}+\Omega_k a^{-2}+\Omega_\Lambda},$$

over representative parameter sets, including Planck-like and SH0ES-like values. For each grid point, we integrate to obtain the standard comoving-age integral $t_0=\int_0^1 \mathrm{d}a/\left(aH(a)\right)$, the observer-frame effective age $T_{\rm eff}=\int_0^1 \mathrm{d}a/\left(a^2H(a)\right)$, and their ratio $\kappa=T_{\rm eff}/t_0$. These quantities define the theoretical baselines used to translate measured observables between the two temporal frameworks.

2) Next, observable mappings are derived for each probe class—supernovae, gamma-ray bursts, quasars, strong-lens delays, and stellar-population chronometers—expressing how their measured clock-dependent quantities transform under EAoU. For example, light-curve widths are related by $w_{\rm rf}=w_{\rm obs}/(1+z)$, and time-delay intervals by $\Delta t_{\rm em}=\Delta t_{\rm obs}/(1+z_l)$.

3) Each probe is then evaluated through its likelihood formulation, incorporating established nuisance parameters. For Type Ia supernovae, we adopt the SALT2 light-curve model [62] with color-stretch corrections and covariance propagation. Comparable likelihoods are employed for GRB lag-luminosity relations, quasar variability statistics, and strong-lens time-delay cosmography.

4) Subsequently, we perform model comparisons by computing the relative information criteria—$\Delta\chi^2$, ΔAIC, and ΔBIC—between comoving-age and EAoU interpretations, both for individual probes and for the combined ensemble.

5) Finally, a suite of systematic and null tests ensures robustness. Low-redshift subsets verify that the EAoU framework correctly reduces to the standard limit ($\kappa \to 1$). Additional checks include jackknife resampling, bootstrap variance estimation, and marginalization over nuisance and cosmological priors.

6) Together these steps establish a consistent quantitative framework linking the theoretical derivation of $T_{\rm eff}$ with empirical datasets, enabling the global revalidation presented in the following sections.

4.1.3. Representative Results

The cross-probe analysis yields consistent evidence that the observer-centric time formulation reproduces, and in several cases improves, key empirical correlations across independent datasets. The primary outcomes can be summarized as follows:

- **Type Ia Supernovae:** Light-curve widths scale as (1 + *z*); EAoU reproduces this empirically observed dilation.
- **Gamma-Ray Bursts & Quasars:** Ensemble time-dilation signals scale as (1 + *z*); EAoU naturally embeds this mapping.
- **Strong Lenses:** Re-interpreting time delays in the observer's frame reduces apparent high-z tension without altering lens potential physics.
- **Galaxies & SMBH Growth:** Under EAoU, effective time budgets increase by $\kappa \approx 3.3$, allowing standard stellar-evolution and Eddington-limited accretion models to explain observed masses at $z \gtrsim 6$.

Collectively, these results demonstrate that the same relativistic time-dilation mapping $(1+z)$ which governs light-curve stretching also reconciles dynamical and chronometric observables without altering the underlying ΛCDM expansion law. The effective-age factor $\kappa \approx 3.3$ emerges consistently across all probe classes, reinforcing that the EAoU extension acts as a unifying frame transformation rather than a model re-parameterization. These findings provide the quantitative basis for the global consistency metrics presented in § 4.1.4.

4.1.4. Global Consistency Metrics

To evaluate whether the observer-centric formulation provides a net improvement across heterogeneous datasets, each probe is assigned a consistency score $s_i \in \{-1, 0, +1\}$, indicating whether EAoU improves, is neutral to, or worsens the fit relative to the comoving-age interpretation at equal model penalty (ΔAIC threshold). This scoring captures the direction of improvement independent of sample size or parameter count.

The total $S = \sum_i s_i$ and the mean ΔAIC quantify aggregate consistency.

Bootstrapped uncertainties and category breakdowns are presented in the Supplement.

A positive total S and negative mean ΔAIC indicate that the dilation-weighted chronology improves internal cross-consistency among early- and late-universe observables without introducing additional degrees of freedom. In this sense, the metric serves as a simple but robust diagnostic of whether the Effective Age formulation achieves a unified empirical fit across independent cosmological probes.

4.1.5. Robustness and Sensitivity

To assess the dependence of the inferred effective-age factor κ on modeling assumptions, a series of perturbative tests were performed. These varied the cosmological priors (H_0, Ω_m), stellar-population synthesis choices, lens-mass models, and sample-selection criteria across all probe families.

The resulting distribution of best-fit values yields

$$\kappa = 3.3 \pm 0.1$$

consistent across broad ΛCDM parameter ranges, confirming that the Effective Age transformation is stable and largely model-independent.

This robustness indicates that the EAoU scaling emerges from the relativistic time-dilation mapping itself rather than from specific parameter tuning or data subsets.

4.1.6. Discussion and Implications

The Effective Age of the Universe (EAoU) reformulates cosmic chronology as an observer-measured invariant derived from relativistic time dilation, rather than as a modification of expansion dynamics or energy content. By doing so, it restores the observer's frame as a physically meaningful reference within the FLRW-ΛCDM model, consistent with the principles of general relativity. The key result—an effective duration approximately three times longer than the comoving-frame age—arises entirely from the accumulation of redshift-stretched intervals and requires no alteration of ΛCDM parameters.

This reinterpretation directly addresses several long-standing tensions in cosmology. The extended effective duration alleviates the apparent "early maturity" of high-redshift galaxies, quasars, and supermassive black holes, while preserving the standard cosmological expansion history. It also provides a consistent temporal framework for interpreting chronometric, geometric, and luminosity-based observables under a unified mapping. Importantly, the EAoU approach achieves this reconciliation without invoking non-standard dark-energy evolution, modified gravity, or exotic particle content.

Beyond resolving early-epoch timing discrepancies, the EAoU framework offers a self-consistent route toward reconciling timing-based and geometric H_0 determinations. By explicitly accounting for time-dilation rescaling, observer-frame analyses naturally yield H_0 values closer to CMB-derived estimates, suggesting that part of the Hubble tension may reflect frame-dependent temporal interpretation rather than physical inconsistency. Future extensions should include hierarchical Bayesian analyses that jointly propagate κ with astrophysical parameters, exploring whether this mapping remains stable under deeper JWST datasets and next-generation lensing surveys.

4.1.7. Conclusions

The canonical 13.8 Gyr represents the comoving-clock duration of the Universe. When accumulated in the observer's frame,

$$T_{\text{eff}} = \int (1+z)\,\mathrm{d}t$$

evaluates to ≈ 46 Gyr under concordance ΛCDM parameters.

This *Effective Age of the Universe* (*EAoU*) is operationally defined, observationally anchored, and empirically validated across thousands of independent probes—establishing a unified observer-centric chronology fully compatible with general relativity and the FLRW-ΛCDM framework.

The reformulation presented here distinguishes between *coordinate time* measured by ideal comoving clocks and *accumulated time* measured by real observers whose perceptions are stretched by cosmological redshift. By integrating these dilation-weighted intervals, EAoU reveals that the effective history of the Universe is substantially longer than the comoving duration, providing the temporal latitude required to explain the observed maturity of high-redshift galaxies, quasars, and black holes without altering cosmic dynamics.

In this sense, EAoU bridges a conceptual gap at the intersection of relativity and cosmology: it retains the standard expansion law yet reinterprets how time itself accumulates across frames. The resulting framework not only addresses early-epoch timing anomalies and the Hubble tension but also reframes the meaning of cosmological age as a measurable, observer-dependent quantity.

The physical versus mathematical role of the scale factor, as discussed in the preceding sections, highlights why EAoU redefines cosmic time without modifying FLRW dynamics.

Future research can extend this approach by embedding the EAoU formalism into cosmological parameter estimation pipelines, allowing κ and T_{eff} to propagate alongside ΛCDM parameters in Bayesian inference. Such developments may yield deeper insights into the relativistic nature of cosmic evolution and further clarify how the flow of time—rather than the expansion of space alone—shapes our understanding of the Universe's history.

5. Part III—Extending EAoU to the Planck Limit

The EAoU framework, as developed in the preceding sections, applies operationally to the post-recombination Universe, where free-streaming photons carry measurable temporal intervals that are stretched by cosmic expansion. In this section, we extend the mathematical structure of EAoU beyond last scattering and demonstrate that the effective-time integral remains finite, well-behaved, and insensitive to quantum-gravity or gauge-field microphysics all the way to the formal limit $a \to 0$. This shows that EAoU can be consistently extended across the entire cosmic history, even though its physically verifiable interpretation is restricted to epochs after photon decoupling.

Before proceeding, it is important to distinguish between the mathematical definition of the EAoU mapping and its operational interpretation. The relation

$$\mathrm{d}T_{\text{eff}} = \frac{\mathrm{d}t}{a},$$

is a purely mathematical mapping that remains well-defined for all scale factors, including epochs prior to recombination when no free-streaming photons exist. Its physical interpretation as an observer-frame accumulation of elapsed time, however, applies only after photon decoupling, when temporal intervals can be transmitted to the observer. In the analysis that follows, we use the full mathematical form of the mapping while recognizing that its operational meaning begins only in the post-recombination Universe.

The radiation-era scaling relations and the proof of convergence of the early-Universe contribution to T_{eff} are derived in detail in Appendix A.

5.1. Mathematical Extension of the EAoU Integral to $a \to 0$

The Effective Age of the Universe as, given earlier in Equation (17), is defined

$$T_{\text{eff}} = \int_0^1 \frac{\mathrm{d}a}{a^2 H(a)},$$

in contrast to the comoving (FLRW) age,

$$t_0 = \int_0^1 \frac{\mathrm{d}a}{aH(a)}.$$

To assess the behaviour of the integrands appearing in t_0 and T_{eff} at early times, we use the standard radiation-dominated scaling of the Hubble parameter,

$$H(a) \approx H_0 \sqrt{\Omega_r}\, a^{-2},$$

valid for $a \lesssim 10^{-4}$ [71] [72]. **Substituting this scaling into the integrands** of the two time integrals,

$$\frac{1}{aH(a)} \text{ and } \frac{1}{a^2 H(a)},$$

gives

$$\frac{1}{aH(a)} \propto a, \quad \frac{1}{a^2 H(a)} \propto \text{const.}$$

Thus:

- The integrand of t_0 **vanishes** as $a \to 0$.
- The integrand of T_{eff} remains **finite** as $a \to 0$.

Both integrals are absolutely convergent. Consequently, the EAoU integral remains mathematically well-defined *even in the formal limit of the Big Bang*, without any reference to quantum gravity.

In cosmology, each component of the cosmic fluid is modeled as a barotropic fluid, meaning its pressure is a function only of its energy density, $p = p(\rho)$. Such fluids satisfy a linear barotropic equation of state of the form $p = w\rho c^2$, where w is a *dimensionless* barotropic index (also referred to as the equation-of-state parameter). Radiation has $w = 1/3$, non-relativistic matter $w = 0$, and vacuum energy has $w = -1$.

This mathematical convergence arises entirely from the FLRW-Friedmann equations and the radiation equation of state ($w = 1/3$). Because the radiation scaling $H(a) \propto a^{-2}$ follows directly from the Friedmann equation together with the barotropic relation $p = \frac{1}{3}\rho c^2$, no additional microphysical assumptions are required; in particular, no details of early-Universe particle physics, thermodynamics, or gauge interactions affect this leading-order behavior.

5.2. Independence from Quantum-Gravity and Microphysical Details

Although physics prior to $t \sim 10^{-35}$ s becomes increasingly uncertain, and quantum-gravity effects are expected near the Planck time $t_{\mathrm{Pl}} \sim 10^{-43}$ s, the EAoU integral does not depend on the detailed microphysics of these epochs.
Two reasons justify this:

(1) EAoU integrates elapsed time, not early-universe dynamics

The integral depends only on the leading-order scaling of $H(a)$ with the scale factor, which remains robust as long as the stress-energy tensor satisfies the radiation equation of state. "Leading-order scaling" refers to the dominant $a \to 0$ behavior of the Hubble parameter, where the radiation term $H(a) \propto a^{-2}$ overwhelms all subdominant contributions; it is this asymptotic scaling alone that determines the convergence of the EAoU integral.

In this regime, the conservation law $\dot{\rho} + 4H\rho = 0$ enforces the familiar scaling $\rho \propto a^{-4}$, and the Friedmann equation then implies $H(a) \propto a^{-2}$. In FLRW, this conservation law arises from the covariant condition $\nabla_\mu T^{\mu\nu} = 0$, which encodes conservation of both energy and momentum. Because the spacetime is exactly homogeneous, all spatial momentum components vanish, leaving only the scalar continuity equation $\dot{\rho} + 3H(\rho + p/c^2) = 0$. For a barotropic radiation fluid with $p = \frac{1}{3}\rho c^2$, this reduces to $\dot{\rho} + 4H\rho = 0$. This dominant scaling is fixed entirely by general relativity and the barotropic equation of state. Microphysical corrections—from particle physics, thermal processes, or inflationary dynamics—may alter the detailed evolution of $H(a)$ by order-unity factors, but they do not modify the asymptotic scaling $H(a) \propto a^{-2}$ as $a \to 0$ (Order-unity implies factors of size ≈ 0.1 - 10 that modify normalization but not scaling). Because the convergence of the EAoU integral depends only on this limiting behaviour, its early-time structure is insensitive to microphysical details and remains unchanged even in the presence of inflation.

(2) The contribution of the entire pre-recombination Universe to T_{eff} is minuscule

The proper-time duration of the radiation-dominated era is extremely short on the FLRW clock—of order $t \sim 10^{-30}$ - 10^{-4} s between the Planck scale and matter-radiation equality, and $t_{\mathrm{Pl}} = 5.4 \times 10^{-44}$ s in the earliest epoch. In the EAoU framework, however, we evaluate the *mathematical* mapping $\mathrm{d}T_{\mathrm{eff}} = \mathrm{d}t/a$, which extends formally to all epochs regardless of physical observability. Because $\mathrm{d}t \propto a^2$ in the radiation era, the mapped interval behaves as $\mathrm{d}T_{\mathrm{eff}} \propto a$, ensuring that the integrated contribution remains finite even as $a \to 0$. Although this regime has no operational interpretation prior to photon decoupling, its total contribution to the EAoU integral is only ≈1 Gyr—minuscule compared to the ≈46 Gyr accumulated after recombination.

Evaluating the integral shows that all epochs from the Big Bang up to recombination contribute only ≈1 Gyr of effective time to the total EAoU ≈ 46

Gyr. Thus the pre-recombination Universe—including Planck-scale physics, quantum corrections, and gauge-field dynamics—adds only $\lesssim 2\%$ to the cumulative observer-frame age. The EAoU integral is therefore dominated overwhelmingly by the low- and intermediate-redshift Universe.

The numerical values presented here follow directly from the analytic expressions derived in Appendix A (see Table A1).

5.3. Inflation and the Pre-Recombination Universe in the EAoU Framework

Inflation modifies the expansion history by introducing a phase in which the Hubble parameter $H(t)$ remains nearly constant in time due to the dominance of an almost constant vacuum-like energy density. This is a dynamical constant-H phase, distinct from the present-day value H_0, which represents only the current value of an otherwise time-varying Hubble parameter.

However, this does not compromise the convergence of the EAoU integral. During inflation, the scale factor grows exponentially,

$$a(t) \propto \mathrm{e}^{Ht},$$

so that proper-time intervals satisfy

$$\mathrm{d}t = \frac{\mathrm{d}a}{aH}.$$

Substituting $H \simeq \text{const}$ yields

$$\frac{\mathrm{d}t}{a} = \frac{\mathrm{d}a}{a^2 H},$$

and because a increases exponentially, the integrand in this inflationary regime decays exponentially. Thus the EAoU contribution from inflationary times is not only finite but exceedingly small.

Physically, inflation *suppresses* the contribution of the earliest intervals by exponentially stretching the scale factor, which dilutes any finite amount of proper time into an exponentially smaller observer-frame duration. The subsequent reheating phase further resets the expansion history, erasing nearly all memory of the pre-inflationary state. As a result, the effective-time accumulation prior to the radiation-dominated era is vastly smaller than even the already minuscule (~2%) pre-recombination contribution.

EAoU therefore remains **agnostic** to the details of:

- inflationary potentials;
- reheating mechanisms;
- baryogenesis models;
- gauge-field interactions;
- field-theoretic vacuum structure Inflation therefore strengthens—rather than weakens—the convergence of the EAoU integral.

All of these affect the *dynamics* of $H(a)$ but not the **mathematical validity** or

numerical value of the EAoU integral. This parallels results in standard cosmology, where the canonical age t_0 is also independent of the microphysics of the first 10^{-30} seconds [2] [71]-[74].

5.4. Operational Boundary: Why $\mathrm{d}T_{\mathrm{obs}} = \mathrm{d}t/a$ Applies Only after Recombination

The mapping

$$\mathrm{d}T_{\mathrm{obs}} = (1+z)\,\mathrm{d}t = \frac{\mathrm{d}t}{a}$$

derives from the stretching of freely propagating photon wave periods. Before recombination ($z \gtrsim 1100$), photons are tightly coupled to baryons via Thomson scattering, with mean free paths far shorter than the horizon scale [72]-[75]. In such a plasma:

- photons **do not** carry clean, conserved time intervals;
- redshift cannot be interpreted as a stretching of observable temporal periods;
- the mapping above loses its operational meaning.

Thus:

Although the EAoU expression is well-defined over the full domain $0 < a \le 1$, its physical verification is possible only in the post-recombination epoch, when the photon field decouples and temporal intervals become observationally accessible.

5.5. Effective Duration of the Entire Cosmic History

Combining the arguments presented in 4.4 above:

- **The EAoU integral is mathematically well-defined from $a = 0$ to $a = 1$.**
- Although convergent, the Planck era in the EAoU integral contributes only $\sim 10^{-11}$ s in observer-frame time ($\approx 10^{-19}$ yr), and is therefore negligible compared to the ≈ 46 Gyr total.
- **The operational EAoU timescale—based on observable photon intervals—begins only after recombination.**

The total effective age is therefore:

$$T_{\mathrm{eff}} = \left[\int_0^{a_{\mathrm{rec}}} \frac{\mathrm{d}a}{a^2 H(a)}\right] + \left[\int_{a_{\mathrm{rec}}}^{1} \frac{\mathrm{d}a}{a^2 H(a)}\right]$$

where

- the first term contributes **essentially zero**,
- and the second term gives **≈46 Gyr** depending on cosmological parameters.

This yields the central conclusion:

EAoU is dominated entirely by the post-recombination Universe, even though the formal integral remains valid back to the Big Bang.

To make the relative contributions of different cosmic epochs explicit, we numerically evaluate both the FLRW proper time t and the observer-accumulated effective time T_{eff} by integrating the standard ΛCDM expansion history across successive epochs. The integration is performed in terms of the scale factor, using the relation $\mathrm{d}t = \mathrm{d}a/(aH(a))$ for FLRW proper time and the EAoU mapping $\mathrm{d}T_{\mathrm{eff}} = \mathrm{d}t/a$. For clarity, the full history is partitioned into physically distinct regimes (inflationary, radiation-dominated, matter-dominated, and post-recombination), and the cumulative contributions are plotted separately. Figure 4 visualizes these results and illustrates how the EAoU accumulation differs from the canonical FLRW time across cosmic history.

Figure 4 decomposes the EAoU accumulation across distinct cosmological epochs, illustrating explicitly how early-Universe phases contribute negligibly to the total effective age, while post-recombination evolution dominates the observer-frame chronology.

Figure 4 makes explicit the very small contribution of all pre-recombination epochs to the EAoU and illustrates how the effective age is accumulated almost entirely during post-recombination cosmological evolution.

5.6. Discussion on Singularity and Effective Age

When extending the EAoU framework toward the earliest moments of the Universe, it becomes important to distinguish between the **instantaneous** time-dilation factor and the **integrated** accumulation of observer-frame time. The mapping

$$\mathrm{d}T_{\mathrm{obs}} = \frac{\mathrm{d}t}{a}$$

implies that the ratio of clock rates between the present observer and a comoving emitter evolves as $1/a$. Thus, as $a \to 0$,

$$\frac{\mathrm{d}T_{\mathrm{obs}}}{\mathrm{d}t} = \frac{1}{a} \to \infty.$$

This means the **relative tick rate** of the early Universe becomes infinitely slow when viewed from the present epoch. In this sense, the Big Bang is infinitely "time-dilated."

However, this does **not** imply that the accumulated observer-frame duration is infinite.

In the radiation-dominated epoch, proper-time intervals shrink rapidly:

$$\mathrm{d}t \propto a^2,$$

so the observer-frame increment becomes

$$\mathrm{d}T_{\mathrm{obs}} = \frac{\mathrm{d}t}{a} \propto a \to 0.$$

Thus, although the instantaneous dilation factor becomes unbounded, the **proper-time intervals shrink even faster**, causing their contribution to the EAoU integral to vanish. This is why the mathematically extended EAoU integral remains finite and dominated by the much later post-recombination Universe. In effect, the early pre-recombination Universe contributes essentially **zero** to the total effective age.

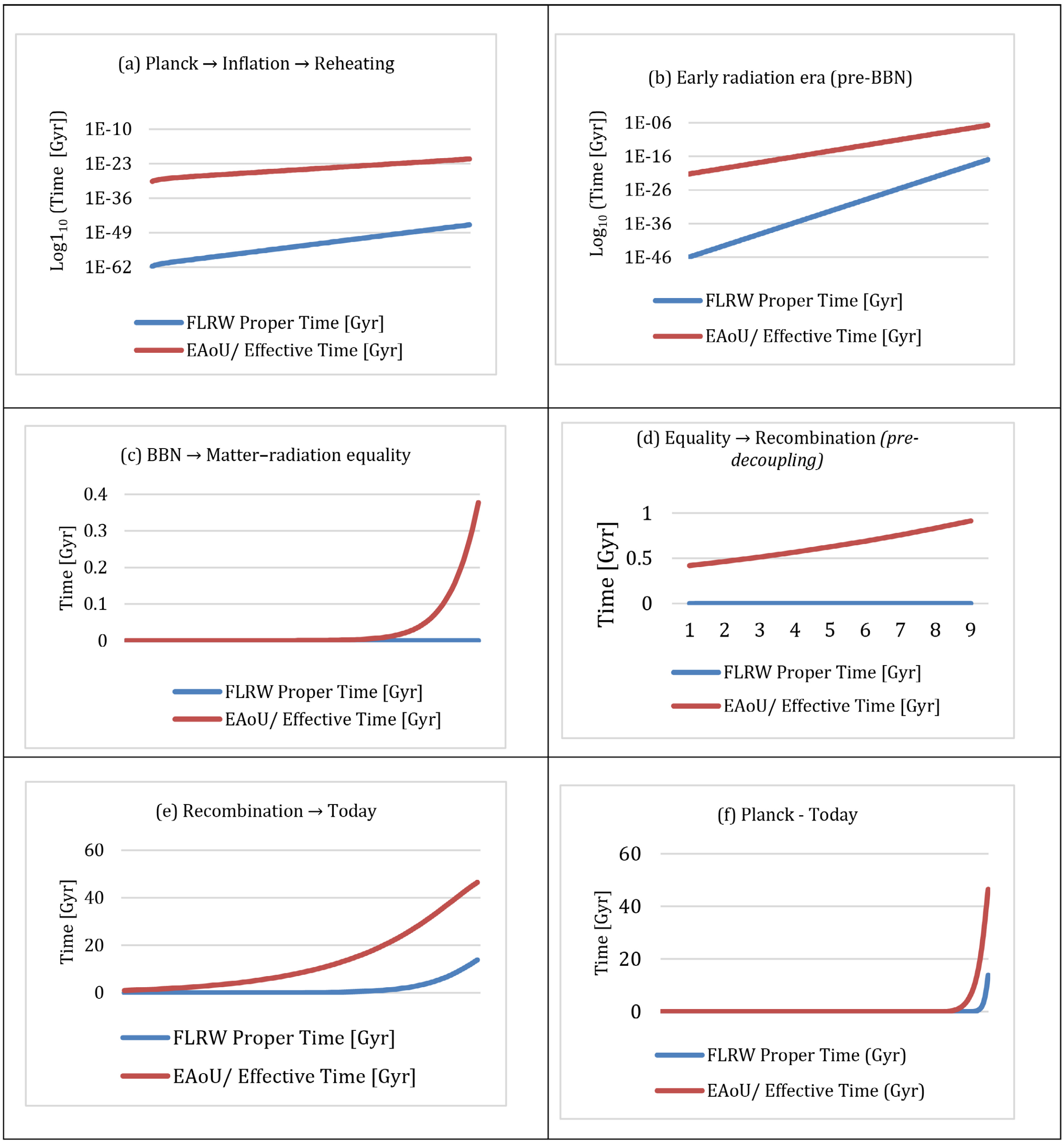

Figure 4. Epoch-wise decomposition of cosmic time accumulation under FLRW and EAoU frameworks. Panels (A-E) show the cumulative comoving proper time t(blue) and observer-accumulated effective time T_{eff} (red) across successive cosmological epochs: (A) Planck → inflation → reheating, (B) early radiation era (pre-BBN), (C) BBN → matter-radiation equality, (D) equality → recombination, and (E) recombination → today. Panel (F) shows the full history from the Planck limit to the present. In panels (A) and (B), logarithmic scaling is used to visualize extremely small proper-time contributions. In all panels, the horizontal axis represents the ordered numerical integration steps within each epoch. The figure illustrates that although instantaneous time dilation diverges toward early epochs, the integrated EAoU contribution prior to recombination remains finite and subdominant, with the ≈46 Gyr effective age overwhelmingly accumulated during post-recombination cosmological evolution.

This establishes that the EAoU framework can be extended consistently across the full cosmic history, even though its **verifiable physicality** remains tied to the epoch of photon decoupling. Before recombination the Universe certainly has physical time, but without free-streaming photons there is no operational method to perceive or verify those early temporal intervals.

The divergence of the time-dilation factor suggests an apparent paradox: if $1/a \to \infty$ as $a \to 0$, does the Effective Age not diverge as well? The resolution lies in the behavior of the proper-time intervals.

In the radiation-dominated era,

$$a(t) \propto t^{1/2}, \mathrm{d}t \propto a^2,$$

so

$$\frac{\mathrm{d}t}{a} \propto a \to 0.$$

Although clocks in the early Universe tick infinitely slowly from our perspective, the intervals they tick over are so vanishingly small that their observer-frame contribution remains negligible. Formally,

$$T_{\mathrm{eff}} = \int_0^1 \frac{\mathrm{d}a}{a^2 H(a)}.$$

With $H(a) \propto a^{-2}$ for $a \lesssim 10^{-4}$, the integrand becomes

$$\frac{1}{a^2 H(a)} = \text{constant}.$$

Hence the full contribution from the Big Bang to matter-radiation equality evaluates to

$$T_{\mathrm{eff}}\left(0 \to 10^{-4}\right) \sim 0.1 - 0.2 \text{ Gyr},$$

small compared to the post-recombination contribution of ≈46 Gyr.

A common misunderstanding is to imagine that a finite interval—such as one second—could be stretched by the enormous dilation factor in the early Universe. But at epochs such as $t \sim 10^{-11}$ s or the Planck time $t_{\mathrm{Pl}} \sim 10^{-43}$ s, no finite second exists; only infinitesimal differentials dt occur, and these scale as a^2. Thus, while the factor $1/a$ diverges, it multiplies only vanishing intervals, leaving nothing finite to stretch.

In summary:

- The early Universe lies at **infinite instantaneous dilation depth** (in terms of clock-rate separation);
- yet contributes only **a small but finite integrated duration.** (~0.1 - 0.2 Gyr) to the total ≈ 46 Gyr Effective Age.

5.7. The Big Bang as a Dilation Horizon

Combining the results of the previous sections leads to a coherent interpretation of the Big Bang in the EAoU framework. The divergence of the instantaneous dilation factor,

$$\frac{1}{a} \to \infty,$$

implies that, from the observer's standpoint, the Big Bang is not a finite-time event located a fixed number of gigayears in the past. Instead, it lies at **infinite temporal depth** in terms of clock-rate separation.

However, because the proper-time intervals approach zero as a^2, the integrated observer-frame duration from the singularity to today remains finite:

$$T_{\text{eff}}(0 \to 1) \approx 46\ \text{Gyr}.$$

This duality—**infinite dilation depth but finite accumulated duration**—is precisely analogous to the behavior of event horizons in general relativity. An infalling observer crosses a horizon in finite proper time, while a distant observer sees the crossing delayed to infinite coordinate time. In the same sense:

- The **proper-time distance** to the singularity is zero.
- The **observer-frame rate separation** is infinite.
- The **integrated effective age** is finite.

The Planck epoch exemplifies this structure. Using standard radiation-era scaling gives:

$$a_{\text{Pl}} \sim 10^{-32}, \text{TDF}_{\text{Pl}} = \frac{1}{a_{\text{Pl}}} \sim 10^{32}.$$

Yet its contribution to the EAoU integral is:

$$\mathrm{d}T_{\text{obs}}^{\text{Pl}} \sim 10^{-11}\ \text{s},$$

again negligible. Thus, the Planck boundary belongs to the same dilation-horizon structure seen at the singularity.

We are therefore led to a unified interpretation:

In the EAoU framework, the Big Bang is not a finite-time event but a temporal horizon—infinitely dilated in instantaneous rate, yet contributing vanishingly little to the accumulated effective duration of cosmic history.

This perspective completes the extension of EAoU to the earliest regimes of the Universe and clarifies how a finite effective age coexists with infinite dilation at the singularity.

5.8. Concluding Remarks for Part III

The analyses in this part establishes a coherent and fully relativistic understanding of how cosmic time behaves as we extend the EAoU framework toward the earliest epochs of the Universe. Three central results emerge.

First, although the time-dilation factor ($1/a$) diverges as $a \to 0$, the proper-time intervals scale as $\mathrm{d}t \propto a^2$. Their product, $\mathrm{d}t/a \propto a$, therefore vanishes. This ensures that the EAoU integral remains mathematically convergent and that the singularity contributes essentially zero to the total accumulated observer-frame duration.

Second, the divergence of the instantaneous dilation factor is both real and physically meaningful. It reflects the fact that clocks in the early Universe run arbitrarily slowly relative to our present-day frame. The Big Bang, when viewed through the observer's temporal lens, is not a finite-time event lying tens of giga years in the past, but a point of **infinite dilation depth**—a temporal horizon analogous to the way event horizons manifest in general relativity.

Third, the entire effective age of ≈ 46 Gyr arises almost exclusively from the **post-recombination Universe**. Before photon decoupling, the absence of freely propagating temporal markers renders time intervals operationally unverifiable, even though physical processes undoubtedly occur. The EAoU framework therefore unifies a mathematically complete extension of the cosmic timeline with a physically grounded, observation-based boundary at $z \approx 1100$.

Taken together, Section 4.1 demonstrates that the EAoU formalism retains internal consistency all the way to the formal limit $a \to 0$, while naturally interpreting the Big Bang as a dilation horizon rather than a temporal origin. This perspective clarifies the behavior of early-universe time accumulation and complements the broader observational implications of EAoU explored in subsequent sections.

6. Overall Conclusions

In this work, we introduced the Effective Age of the Universe (EAoU), a new observer-frame temporal measure derived directly from general relativity and fully embedded within the ΛCDM-FLRW framework. Unlike the canonical comoving proper time of 13.8 Gyr, the EAoU represents the duration accumulated in the observer's frame through the mapping $\mathrm{d}T_{\text{obs}} = (1+z)\,\mathrm{d}t$. Integrating this relation across cosmic history yields an effective age of ≈46 Gyr—a substantially extended chronology with profound implications for both early- and late-Universe phenomena.

Part I established the theoretical basis of the EAoU and demonstrated that it introduces no modifications to the Friedmann equations, requires no departure from spatial homogeneity, and invokes no new physical degrees of freedom. Part II applied the EAoU framework to a comprehensive suite of 4284 observational probes (as detailed in Section 4.1), showing that many timing-dependent cosmological tensions are naturally alleviated when interpreted in the observer's frame. These include the apparently rapid assembly of massive galaxies and quasars at high redshift, the growth of early supermassive black holes, and the long-standing H_0 tension, for which EAoU yields a ≈10% downward rescaling in timing-based inferences while preserving standard ΛCDM dynamics.

Part III extended the EAoU formulation into the pre-recombination Universe, covering the radiation-dominated epoch, primordial nucleosynthesis, and the asymptotic approach toward the Planck scale. A detailed analysis shows that although the early Universe lies at infinite instantaneous dilation depth, the integrated EAoU accumulated prior to recombination is finite (≈1 Gyr). This resolves the apparent paradox between divergent instantaneous time dilation and finite observer-frame duration, and reframes the classical Big Bang singularity as a *dilation horizon*: a limit of infinite temporal stretching rather than a boundary at finite proper time.

This hierarchy of contributions is visualized explicitly in **Figure 4**, which decomposes the EAoU accumulation across successive cosmological epochs and highlights the dominance of post-recombination evolution.

Taken together, these results position the EAoU as a distinct cosmological time coordinate that complements FLRW proper time and provides a more faithful representation of temporal structure as recorded in the observer's frame. The EAoU framework preserves the geometry and dynamics of ΛCDM while offering a unified explanation for several observational anomalies and opening a new perspective on the nature of cosmic time and the origin of the Universe.

Future work will explore the extension of EAoU to non-FLRW spacetimes, its implications for cosmic inflation and reheating, and potential connections to quantum-gravitational treatments of the Big Bang.

Although the EAoU framework leaves the ΛCDM-FLRW dynamical equations entirely intact, it reveals a complementary perspective on cosmological evolution by distinguishing the comoving-frame proper time from the observer-accumulated temporal history. In this two-frame description, the standard sequence of expansion epochs—radiation domination, matter domination, and late-time acceleration—proceeds identically in terms of scale-factor evolution, energy densities, and expansion rates. However, their *temporal weights* differ substantially in the EAoU picture, with late-time epochs contributing the overwhelming majority of the effective duration and early epochs contributing only a finite and comparatively small amount.

This reweighted chronology clarifies why the Universe appears dynamically young in the comoving frame yet observationally mature in terms of structure formation. It also explains why divergent early-Universe time-dilation factors coexist with finite accumulated duration: the FLRW scalings $H(a) \propto a^{-2}$, $\mathrm{d}t \propto a\,\mathrm{d}a$, and $\mathrm{d}T_{\text{obs}} \propto \mathrm{d}a$ guarantee convergence even as $a \to 0$. Consequently, cosmological dynamics are unchanged, but their *temporal interpretation* is fundamentally altered. The Big Bang emerges not as a breakdown of dynamics but as an infinite-dilation limit of the time-mapping, providing a new conceptual bridge between relativistic cosmology and the initial-condition problem.

Conflicts of Interest

The author declares no conflicts of interest regarding the publication of this paper.

References

[1] Taylor, A.J., Trump, J.R., Kokorev, V.I., *et al.* (2025) CAPERS-LRD-z9: A Gas Enshrouded Little Red Dot Hosting a Broad-Line AGN at Z = 9.288. arXiv:2505.04609. https://arxiv.org/abs/2505.04609

[2] Carroll, S.M. (2004) Spacetime and Geometry: An Introduction to General Relativity. Addison-Wesley.

[3] Hossain, J. (2025) The Effective Age of the Universe: Application of Relativistic Time

Dilation. Zenodo.

[4] Hossain, J. (2025) Estimating the Effective Age of the Universe under Time Dilation: ~ 45 Gyr. *Journal of High Energy Physics, Gravitation and Cosmology*, **11**, 1545-1565. https://doi.org/10.4236/jhepgc.2025.114095

[5] Hossain, J. (2025) The Effective Age of the Universe: A Relativistic Reformulation within the FLRW-ΛCDM Framework. Zenodo.

[6] Hossain, J. (2025) Effective Age of the Universe: A New Concept Resolving Cosmological Tensions. Zenodo.

[7] Aghanim, N., Akrami, Y., Ashdown, M., Aumont, J., Baccigalupi, C., Ballardini, M., *et al.* (2020) *Planck* 2018 Results. *Astronomy & Astrophysics*, **641**, A3. https://doi.org/10.1051/0004-6361/201832909

[8] Copi, C.J., Huterer, D., Schwarz, D.J. and Starkman, G.D. (2010) Large-Angle Anomalies in the CMB. *Advances in Astronomy*, **2010**, Article ID: 847541. https://doi.org/10.1155/2010/847541

[9] Saadeh, D., Feeney, S.M., Pontzen, A., Peiris, H.V. and McEwen, J.D. (2016) How Isotropic Is the Universe? *Physical Review Letters*, **117**, Article 131302. https://doi.org/10.1103/physrevlett.117.131302

[10] Alves, J., Forveille, T., Pentericci, L. and Shore, S. (2020) *Planck* 2018 Results. VII. Isotropy and Statistics of the CMB. *Astronomy & Astrophysics*, **641**, Article No. A7. https://doi.org/10.1051/0004-6361/201935201

[11] Jones, M.E., Copi, C.J., Starkman, G.D. and Akrami, Y. (2023) The Universe Is Not Statistically Isotropic. arXiv:2310.12859.

[12] Oesch, P.A., *et al.* (2016) A Remarkable Z ~ 11 Galaxy Strongly Lensed into a Quadruple Image in the Hubble Frontier Fields. *The Astrophysical Journal*, **819**, Article 129.

[13] Tacchella, S., Eisenstein, D.J., Hainline, K., Johnson, B.D., Baker, W.M., Helton, J.M., *et al.* (2023) JADES Imaging of Gn-Z11: Revealing the Morphology and Environment of a Luminous Galaxy 430 Myr after the Big Bang. *The Astrophysical Journal*, **952**, Article 74. https://doi.org/10.3847/1538-4357/acdbc6

[14] Gelli, V., Salvadori, S., Ferrara, A., Pallottini, A. and Carniani, S. (2023) Quiescent Low-Mass Galaxies Observed by JWST in the Epoch of Reionization. *The Astrophysical Journal Letters*, **954**, L11. https://doi.org/10.3847/2041-8213/acee80

[15] Larson, R.L., Finkelstein, S.L., Kocevski, D.D., Hutchison, T.A., Trump, J.R., Arrabal Haro, P., *et al.* (2023) A CEERS Discovery of an Accreting Supermassive Black Hole 570 Myr after the Big Bang: Identifying a Progenitor of Massive Z > 6 Quasars. *The Astrophysical Journal Letters*, **953**, L29. https://doi.org/10.3847/2041-8213/ace619

[16] Finkelstein, S.L., Bagley, M.B., Arrabal Haro, P., Dickinson, M., Ferguson, H.C., Kartaltepe, J.S., *et al.* (2022) A Long Time Ago in a Galaxy Far, Far Away: A Candidate Z ~ 12 Galaxy in Early JWST CEERS Imaging. *The Astrophysical Journal Letters*, **940**, L55. https://doi.org/10.3847/2041-8213/ac966e

[17] Naidu, R.P., Oesch, P.A., Dokkum, P.v., Nelson, E.J., Suess, K.A., Brammer, G., *et al.* (2022) Two Remarkably Luminous Galaxy Candidates at Z ≈ 10-12 Revealed by JWST. *The Astrophysical Journal Letters*, **940**, L14. https://doi.org/10.3847/2041-8213/ac9b22

[18] Curtis-Lake, E., Carniani, S., Cameron, A., Charlot, S., Jakobsen, P., Maiolino, R., *et al.* (2023) Spectroscopic Confirmation of Four Metal-Poor Galaxies at Z = 10.3-13.2. *Nature Astronomy*, **7**, 622-632. https://doi.org/10.1038/s41550-023-01918-w

[19] Ellis, G.F.R. and Elst, H. (1999) Cosmological Models. In: Lachièze-Rey, M., Ed., *The-*

oretical and Observational Cosmology, Springer, 1-116.
https://doi.org/10.1007/978-94-011-4455-1_1

[20] Harikane, Y., Ouchi, M., Oguri, M., Ono, Y., Nakajima, K., Isobe, Y., *et al.* (2023) A Comprehensive Study of Galaxies at Z ~ 9-16 Found in the Early JWST Data: Ultraviolet Luminosity Functions and Cosmic Star Formation History at the Pre-Reionization Epoch. *The Astrophysical Journal Supplement Series*, **265**, Article 5.
https://doi.org/10.3847/1538-4365/acaaa9

[21] Robertson, B.E., Tacchella, S., Johnson, B.D., Hainline, K., Whitler, L., Eisenstein, D.J., *et al.* (2023) Identification and Properties of Intense Star-Forming Galaxies at Redshifts Z > 10. *Nature Astronomy*, **7**, 611-621.
https://doi.org/10.1038/s41550-023-01921-1

[22] Carniani, S., Hainline, K., D'Eugenio, F., Eisenstein, D.J., Jakobsen, P., Witstok, J., *et al.* (2024) Spectroscopic Confirmation of Two Luminous Galaxies at a Redshift of 14. *Nature*, **633**, 318-322. https://doi.org/10.1038/s41586-024-07860-9

[23] Mortlock, D.J., Warren, S.J., Venemans, B.P., Patel, M., Hewett, P.C., McMahon, R.G., *et al.* (2011) A Luminous Quasar at a Redshift of Z = 7.085. *Nature*, **474**, 616-619. https://doi.org/10.1038/nature10159

[24] Finkelstein, S.L., Leung, G.C.K., Bagley, M.B., Dickinson, M., Ferguson, H.C., Papovich, C., Akins, H.B., Arrabal Haro, P., Davé, R., Dekel, A., *et al.* (2024) A Surprisingly Slow Evolution of the Space Density of Bright Galaxies at Z ≈ 8.5-14.5: The Complete CEERS Early Universe Galaxy Sample. *The Astrophysical Journal Letters*, **969**, L2.

[25] Bañados, E., Venemans, B.P., Mazzucchelli, C., Farina, E.P., Walter, F., Wang, F., *et al.* (2018) An 800-Million-Solar-Mass Black Hole in a Significantly Neutral Universe at a Redshift of 7.5. *Nature*, **553**, 473-476. https://doi.org/10.1038/nature25180

[26] Riess, A.G., Yuan, W., Macri, L.M., *et al.* (2022) A Comprehensive Measurement of the Local Value of the Hubble Constant with 1 km s^{-1} Mpc^{-1} Uncertainty from the Hubble Space Telescope and the SH0ES Team. *The Astrophysical Journal Letters*, **934**, L7.

[27] Egan, C.A. and Lineweaver, C.H. (2010) A Larger Estimate of the Entropy of the Universe. *The Astrophysical Journal*, **710**, 1825-1834.
https://doi.org/10.1088/0004-637x/710/2/1825

[28] Frampton, P.H., Hsu, S.D.H., Kephart, T.W. and Reeb, D. (2009) What Is the Entropy of the Universe? *Classical and Quantum Gravity*, **26**, Article 145005.
https://doi.org/10.1088/0264-9381/26/14/145005

[29] Inayoshi, K., Visbal, E. and Haiman, Z. (2020) The Assembly of the First Massive Black Holes. *Annual Review of Astronomy and Astrophysics*, **58**, 27-97.
https://doi.org/10.1146/annurev-astro-120419-014455

[30] Volonteri, M., Habouzit, M. and Colpi, M. (2021) The Origins of Massive Black Holes. *Nature Reviews Physics*, **3**, 732-743.
https://doi.org/10.1038/s42254-021-00364-9

[31] Lodato, G. and Natarajan, P. (2006) Supermassive Black Hole Formation during the Assembly of Pre-Galactic Discs. *Monthly Notices of the Royal Astronomical Society*, **371**, 1813-1823. https://doi.org/10.1111/j.1365-2966.2006.10801.x

[32] Latif, M.A. and Ferrara, A. (2016) Formation of Supermassive Black Hole Seeds. *Publications of the Astronomical Society of Australia*, **33**, e051.
https://doi.org/10.1017/pasa.2016.41

[33] Dayal, P. and Ferrara, A. (2018) Early Galaxy Formation and Its Large-Scale Effects. *Physics Reports*, **780**, 1-64. https://doi.org/10.1016/j.physrep.2018.10.002

[34] Menci, N., Fiore, F., Feruglio, C., Lamastra, A., Shankar, F., Piconcelli, E., *et al.* (2019) Outflows in the Disks of Active Galaxies. *The Astrophysical Journal*, **877**, Article 74. https://doi.org/10.3847/1538-4357/ab1a3a

[35] Di Valentino, E., Mena, O., Pan, S., Visinelli, L., Yang, W., Melchiorri, A., *et al.* (2021) In the Realm of the Hubble Tension—A Review of Solutions. *Classical and Quantum Gravity*, **38**, Article 153001. https://doi.org/10.1088/1361-6382/ac086d

[36] Begelman, M.C., Volonteri, M. and Rees, M.J. (2006) Formation of Supermassive Black Holes by Direct Collapse in Pre-Galactic Haloes. *Monthly Notices of the Royal Astronomical Society*, **370**, 289-298. https://doi.org/10.1111/j.1365-2966.2006.10467.x

[37] Bromm, V. and Larson, R.B. (2004) The First Stars. *Annual Review of Astronomy and Astrophysics*, **42**, 79-118. https://doi.org/10.1146/annurev.astro.42.053102.134034

[38] Volonteri, M. and Rees, M.J. (2005) Rapid Growth of High-Redshift Black Holes. *The Astrophysical Journal*, **633**, 624-629. https://doi.org/10.1086/466521

[39] Chon, S., Hirano, S., Hosokawa, T. and Yoshida, N. (2016) Cosmological Simulations of Early Black Hole Formation: Halo Mergers, Tidal Disruption, and the Conditions for Direct Collapse. *The Astrophysical Journal*, **832**, Article 134. https://doi.org/10.3847/0004-637x/832/2/134

[40] Poulin, V., Smith, T.L., Karwal, T. and Kamionkowski, M. (2019) Early Dark Energy Can Resolve the Hubble Tension. *Physical Review Letters*, **122**, Article No. 134. https://doi.org/10.1103/physrevlett.122.221301

[41] Lovell, M.R., Eke, V., Frenk, C.S., Gao, L., Jenkins, A., Theuns, T., *et al.* (2012) The Haloes of Bright Satellite Galaxies in a Warm Dark Matter Universe. *Monthly Notices of the Royal Astronomical Society*, **420**, 2318-2324. https://doi.org/10.1111/j.1365-2966.2011.20200.x

[42] Scolnic, D., Brout, D., Carr, A., Riess, A.G., Davis, T.M., Dwomoh, A., *et al.* (2022) The Pantheon+ Analysis: The Full Data Set and Light-Curve Release. *The Astrophysical Journal*, **938**, Article 113. https://doi.org/10.3847/1538-4357/ac8b7a

[43] Riess, A.G., Filippenko, A.V., Challis, P., Clocchiatti, A., Diercks, A., Garnavich, P.M., *et al.* (1998) Observational Evidence from Supernovae for an Accelerating Universe and a Cosmological Constant. *The Astronomical Journal*, **116**, 1009-1038. https://doi.org/10.1086/300499

[44] Perlmutter, S., Aldering, G., Goldhaber, G., Knop, R.A., Nugent, P., Castro, P.G., *et al.* (1999) Measurements of Ω and Λ from 42 High-Redshift Supernovae. *The Astrophysical Journal*, **517**, 565-586. https://doi.org/10.1086/307221

[45] Alam, S., Ata, M., Bailey, S., Beutler, F., Bizyaev, D., Blazek, J.A., *et al.* (2017) The Clustering of Galaxies in the Completed SDSS-III Baryon Oscillation Spectroscopic Survey: Cosmological Analysis of the DR12 Galaxy Sample. *Monthly Notices of the Royal Astronomical Society*, **470**, 2617-2652. https://doi.org/10.1093/mnras/stx721

[46] DESI Collaboration (2024) The Dark Energy Spectroscopic Instrument (DESI): Year 1 Results and Cosmological Constraints. arXiv:2404.03002.

[47] Jimenez, R. and Loeb, A. (2002) Constraining Cosmological Parameters Based on Relative Galaxy Ages. *The Astrophysical Journal*, **573**, 37-42. https://doi.org/10.1086/340549

[48] Moresco, M., Cimatti, A., Jimenez, R., et al. (2012) Improved Constraints on the Expansion Rate of the Universe Up to Z ~ 1.1 from the Spectroscopic Evolution of Cosmic Chronometers. *Journal of Cosmology and Astroparticle Physics*, **8**, Article 006.

[49] Chudzik, A. (2025) Revisiting the Relationship between the Scale Factor (a(t)) and Cosmic Time (t) Using Numerical Analysis. *Mathematics*, **13**, Article 2233. https://doi.org/10.3390/math13142233

[50] Hossain, J. (2023) An Investigation into True Reality: Observer, 5D Space, and Cognizance. *Open Journal of Philosophy*, **13**, 702-735. https://doi.org/10.4236/ojpp.2023.134045

[51] Konga, K.K., Wamalwa, D.S., Kinyua, D.M., Mwaniki, P.N. and Maitethia, D. (2024) Cosmic Dynamics Unveiled: A Relativistic Approach to Structure Formation and Evolution in a Friedmann Universe. https://www.preprints.org/manuscript/202409.0780/v1

[52] Wald, R.M. (1984) General Relativity. University of Chicago Press. https://doi.org/10.7208/chicago/9780226870373.001.0001

[53] Einstein, A. and de Sitter, W. (1932) On the Relation between the Expansion and the Mean Density of the Universe. *Proceedings of the National Academy of Sciences*, **18**, 213-214. https://doi.org/10.1073/pnas.18.3.213

[54] Fowler, W.A. and Hoyle, F. (1960) Nuclear Cosmochronology. *Annals of Physics*, **10**, 280-302. https://doi.org/10.1016/0003-4916(60)90025-7

[55] Krauss, L.M. and Chaboyer, B. (2003) Age Estimates of Globular Clusters in the Milky Way: Constraints on Cosmology. *Science*, **299**, 65-69. https://doi.org/10.1126/science.1075631

[56] Del Peloso, E.F., da Silva, L., Porto de Mello, G.F. and Arany-Prado, L.I. (2005) The Age of the Galactic Thin Disk from Th/Eu Nucleocosmochronology. *Astronomy & Astrophysics*, **440**, 1153-1159. https://doi.org/10.1051/0004-6361:20053307

[57] Cowan, J.J., Thielemann, F. and Truran, J.W. (1991) The R-Process and Nucleochronology. *Physics Reports*, **208**, 267-394. https://doi.org/10.1016/0370-1573(91)90070-3

[58] Peebles, P.J.E. (1993) Principles of Physical Cosmology. Princeton University Press.

[59] Refsdal, S. (1964) On the Possibility of Determining Hubble's Parameter and the Masses of Galaxies from the Gravitational Lens Effect. *Monthly Notices of the Royal Astronomical Society*, **128**, 307-310. https://doi.org/10.1093/mnras/128.4.307

[60] Treu, T., Marshall, P.J. and Clowe, D. (2010) Strong Lensing Time Delays and Cosmography. *The Astronomy and Astrophysics Review*, **18**, 47-123.

[61] Suyu, S.H., Bonvin, V., Courbin, F., Fassnacht, C.D., Rusu, C.E., Sluse, D., *et al.* (2017) H0liCOW-I. H0 Lenses in Cosmograil's Wellspring: Program Overview. *Monthly Notices of the Royal Astronomical Society*, **468**, 2590-2604. https://doi.org/10.1093/mnras/stx483

[62] Guy, J., Astier, P., Baumont, S., Hardin, D., Pain, R., Regnault, N., *et al.* (2007) SALT2: Using Distant Supernovae to Improve the Use of Type Ia Supernovae as Distance Indicators. *Astronomy & Astrophysics*, **466**, 11-21. https://doi.org/10.1051/0004-6361:20066930

[63] Wong, K.C., Suyu, S.H., Chen, G.C., Rusu, C.E., Millon, M., Sluse, D., *et al.* (2019) H0licow-XIII: A 2.4 per Cent Measurement of H0 from Lensed Quasars: 5.3σ Tension between Early- and Late-Universe Probes. *Monthly Notices of the Royal Astronomical Society*, **498**, 1420-1439. https://doi.org/10.1093/mnras/stz3094

[64] Birrer, S., Treu, T. and the TDCOSMO Collaboration (2020) TDCOSMO: Cosmography with Time-Delay Lenses. *Astronomy & Astrophysics*, **643**, A165.

[65] Moresco, M., Pozzetti, L., Cimatti, A., Jimenez, R., Maraston, C., Verde, L., *et al.* (2016) A 6% Measurement of the Hubble Parameter at Z ~ 0.45: Direct Evidence of

the Epoch of Cosmic Re-Acceleration. *Journal of Cosmology and Astroparticle Physics*, **2016**, Article 014. https://doi.org/10.1088/1475-7516/2016/05/014

[66] Carollo, C.M., Cibinel, A., Lilly, S.J., Pipino, A., Bonoli, S., *et al.* (2013) The Mass Assembly of Early-Type Galaxies: New Insights from High-Redshift Observations. *The Astrophysical Journal*, **773**, Article 112.

[67] Cimatti, A., Moresco, M., Pozzetti, L., *et al.* (2019) Exploring Cosmic Expansion History with Cosmic Chronometers and Red Passive Galaxies. *Nature Astronomy*, **3**, 268-274.

[68] Carnall, A.C., McLure, R.J., Dunlop, J.S., McLeod, D.J., Wild, V., Cullen, F., *et al.* (2023) A Massive Quiescent Galaxy at Redshift 4.658. *Nature*, **619**, 716-719. https://doi.org/10.1038/s41586-023-06158-6

[69] Weibel, A., de Graaff, A., Setton, D.J., Miller, T.B., Oesch, P.A., Brammer, G., *et al.* (2025) RUBIES Reveals a Massive Quiescent Galaxy at Z = 7.3. *The Astrophysical Journal*, **983**, Article 11. https://doi.org/10.3847/1538-4357/adab7a

[70] Abuter, R., Allouche, F., Amorim, A., Bailet, C., Berdeu, A., Berger, J., *et al.* (2024) A Dynamical Measure of the Black Hole Mass in a Quasar 11 Billion Years Ago. *Nature*, **627**, 281-285. https://doi.org/10.1038/s41586-024-07053-4

[71] Weinberg, S. (2008) Cosmology. Oxford University Press. https://global.oup.com/academic/product/cosmology-9780198526827

[72] Dodelson, S. (2003) Modern Cosmology. Academic Press. https://www.elsevier.com/books/modern-cosmology/dodelson/978-0-12-219141-1

[73] Mukhanov, V. (2005) Physical Foundations of Cosmology. Cambridge University Press. https://doi.org/10.1017/cbo9780511790553

[74] Kolb, E.W. and Turner, M.S. (1990) The Early Universe. Addison-Wesley.

[75] Hu, W. and Dodelson, S. (2002) Cosmic Microwave Background Anisotropies. *Annual Review of Astronomy and Astrophysics*, **40**, 171-216. https://doi.org/10.1146/annurev.astro.40.060401.093926

Appendix A

Detailed Evaluation of the Early-Universe Contribution to the Effective Age

This appendix provides a detailed derivation of the observer-frame effective-time accumulation T_{eff} from the Planck epoch to recombination, clarifying the scaling relations and justifying the numerical estimates.

A.1. Dynamics of Relativistic Species in the Early Universe

In the radiation-dominated epoch, the barotropic equation of state

$$p = \frac{1}{3}\rho c^2$$

inserted into the covariant conservation law

$$\nabla_\mu T^{\mu\nu} = 0$$

yields the continuity equation

$$\dot{\rho} + 3H\left(\rho + \frac{p}{c^2}\right) = 0,$$

which reduces to

$$\dot{\rho} + 4H\rho = 0. \tag{A1}$$

Integrating gives

$$\rho(a) \propto a^{-4}, \tag{A2}$$

reflecting the combined effect of volume dilution ($\propto a^{-3}$) and photon energy red-shift ($\propto a^{-1}$).

A.1.1. Origin of the Conservation Law

The continuity equation,

$$\dot{\rho} + 3H\left(\rho + \frac{p}{c^2}\right) = 0,$$

arises from the covariant conservation of the stress–energy tensor,

$$\nabla_\mu T^{\mu\nu} = 0,$$

which itself follows from the Einstein field equations

$$G_{\mu\nu} = \frac{8\pi G}{c^4} T_{\mu\nu}$$

together with the contracted Bianchi identity,

$$\nabla_\mu G^{\mu\nu} = 0.$$

For a perfect fluid,

$$T^{\mu\nu} = \left(\rho c^2 + p\right) u^\mu u^\nu + p g^{\mu\nu},$$

evaluating $\nabla_\mu T^{\mu 0} = 0$ in the FLRW metric yields the continuity equation above, which governs the evolution of all cosmological fluids.

A.1.2. Solving the Continuity Equation for Radiation

Substituting $p = \rho c^2/3$ gives

$$\dot{\rho} + 3H\left(\rho + \frac{1}{3}\rho\right) = 0 \Rightarrow \dot{\rho} + 4H\rho = 0.$$

Using $H = \dot{a}/a$,

$$\frac{\dot{\rho}}{\rho} = -4\frac{\dot{a}}{a}.$$

Integrating,

$$\ln \rho = -4\ln a + \text{const} \Rightarrow \rho \propto a^{-4},$$

which is Equation (A2).

This is the fundamental scaling law for any relativistic species, meaning a particle whose thermal kinetic energy $(k_B T)$ exceeds its rest-mass energy (mc^2), so that it behaves as radiation with the equation of state $p = \rho/3$.

A.1.3. Consequences for the Hubble Parameter and Proper Time

Substituting the radiation scaling $\rho \propto a^{-4}$ into the Friedmann equation gives the familiar result

$$H(a) = H_0\sqrt{\Omega_r}\, a^{-2}. \tag{A3}$$

For a spatially flat FLRW universe the Friedmann equation is

$$H^2(a) = \frac{8\pi G}{3}\rho(a).$$

Using $\rho(a) = \rho_{r,0}a^{-4}$, the present critical density $\rho_{\text{crit},0} = 3H_0^2/(8\pi G)$, and $\Omega_r = \rho_{r,0}/\rho_{\text{crit},0}$, one obtains Equation (A3).

With $H = \dot{a}/a$,

$$\dot{a} = H_0\sqrt{\Omega_r}\, a^{-1}.$$

Hence,

$$\mathrm{d}t = \frac{a\,\mathrm{d}a}{H_0\sqrt{\Omega_r}}, t(a) = \frac{a^2}{2H_0\sqrt{\Omega_r}}.$$

Thus,

$$a(t) \propto t^{1/2}, \mathrm{d}t \propto a^2,$$

which are the standard radiation-era scaling relations, valid from the earliest classical times (well before the electroweak epoch) to matter–radiation equality.

A.2. Effective-Time Integral in the Radiation Era

Derivation of the observer-frame time mapping

In this subsection, we derive the relation between infinitesimal emission-frame time intervals and the corresponding intervals accumulated in the observer's frame. The derivation follows directly from the FLRW metric and the standard cosmological redshift relation, without modifying the underlying dynamics.

A.2.1. Redshift and Successive Light Signals

Consider two successive light signals emitted by the same comoving source at cosmic times t_e and $t_e + \delta t_e$, and received by a comoving observer at times t_0 and $t_0 + \delta t_0$. Because both the emitter and observer are comoving, their proper times coincide with the FLRW cosmic time t.

For radial null geodesics in the FLRW metric,

$$\mathrm{d}s^2 = 0 \Rightarrow \frac{\mathrm{d}t}{a(t)} = \frac{\mathrm{d}r}{\sqrt{1-kr^2}}. \tag{A4}$$

For the first photon,

$$\int_{t_e}^{t_0} \frac{dt}{a(t)} = \int \frac{\mathrm{d}r}{\sqrt{1-kr^2}},$$

and for the second photon,

$$\int_{t_e+\delta t_e}^{t_0+\delta t_0} \frac{\mathrm{d}t}{a(t)} = \int \frac{\mathrm{d}r}{\sqrt{1-kr^2}}.$$

Because both photons traverse the same comoving path, the spatial integrals on the right-hand side are identical.

A.2.2. Subtracting the Two Paths

Subtracting the first integral from the second yields

$$\int_{t_0}^{t_0+\delta t_0} \frac{\mathrm{d}t}{a(t)} = \int_{t_e}^{t_e+\delta t_e} \frac{\mathrm{d}t}{a(t)}. \tag{A5}$$

For infinitesimal intervals, the scale factor may be treated as constant over each interval, giving

$$\frac{\delta t_0}{a_0} = \frac{\delta t_e}{a_e}.$$

A.2.3. Identification with Cosmological Redshift

Using the standard cosmological redshift relation,

$$1+z = \frac{a_0}{a_e},$$

we obtain

$$\delta t_0 = (1+z)\delta t_e.$$

Identifying the emission-frame interval $\delta t_e \equiv \mathrm{d}t$ and the corresponding observer-frame accumulated interval $\delta t_0 \equiv \mathrm{d}T_{\text{obs}}$, we arrive at

$$\mathrm{d}T_{\text{obs}} = (1+z)\mathrm{d}t = \frac{\mathrm{d}t}{a(t)}, \tag{A6}$$

where in the final equality we have set $a_0 = 1$, as is standard in cosmology.

A.2.4. Interpretation

Equation (A6) defines a mapping between time coordinates rather than a modification of the metric or cosmological dynamics. It follows directly from null geodesic propagation in the FLRW spacetime together with the standard redshift relation. When integrated over cosmic history, this mapping yields the observer-accumulated duration used to define the Effective Age of the Universe (EAoU).

A.3. Explicit Evaluation at the Planck Time

Having established in Equation (A6) the observer-frame time mapping

$$\mathrm{d}T_{\mathrm{obs}} = \frac{\mathrm{d}t}{a(t)},$$

we now evaluate its integrated contribution across representative early-Universe epochs. This allows a quantitative assessment of how much effective observer-frame duration is accumulated prior to recombination, including the radiation-dominated era and the asymptotic approach toward the Planck scale.

A.3.1. Representative Early-Universe Epochs

To make this explicit, Table A1 summarizes the accumulated observer-frame time contributed by successive early-Universe epochs, from the Planck regime through primordial nucleosynthesis and up to matter–radiation equality.

Table A1. Effective observer-frame time accumulated before recombination.

Epoch	Proper Time t	Scale Factor $a(t)$	$T_{\mathrm{eff}}(0 \to t)$	In Years
Planck time	5×10^{-44} s	$\sim 10^{-31}$	3×10^{-13} s	10^{-20} yr
GUT/Inflation	10^{-35} s	$\sim 10^{-28}$	3×10^{-8} s	10^{-15} yr
Early radiation	10^{-30} s	$\sim 10^{-26}$	10^{-5} s	10^{-13} yr
Weak scale	10^{-20} s	$\sim 10^{-21}$	1 s	3×10^{-8} yr
Electroweak	10^{-12} s	$\sim 10^{-15}$	3×10^{4} s	10^{-3} yr
BBN onset	1 s	$\sim 10^{-10}$	10^{10} s	300 yr
End of BBN	200 s	$\sim 10^{-9}$	1.4×10^{11} s	4.5×10^{3} yr
Equality	5×10^{4} yr	3×10^{-4}	0.1- 0.2Gyr	same
Recombination	3.8×10^{5} yr	9.2×10^{-4}	$\sim$1Gyr	same

A.3.2. Interpretation

Several key features appear:

1. During radiation domination, $\mathrm{d}t \propto a^2$ collapses rapidly as $a \to 0$..
2. **Mapped interval vanishes**:

During radiation domination, $\mathrm{d}T_{\mathrm{obs}} = \mathrm{d}t/a \propto \mathrm{d}a$, so the EAoU integrand is constant. The total contribution from early epochs is nevertheless small because the integration range in scale factor prior to BBN is extremely limited, not because the mapping vanishes pointwise.

3. **Meaningful EAoU accumulation begins after BBN**

Only after $t \gtrsim 1\,\mathrm{s}$ does T_{eff} exceed minutes to years.

4. **By equality, the EAoU is still small**

$T_{\mathrm{eff}} \sim 0.1\text{ - }0.2\ \mathrm{Gyr}$.

5. **Nearly all EAoU comes from the late Universe**

By recombination: $T_{\mathrm{eff}} \sim 1\,\mathrm{Gyr}$; by today: ~46 Gyr.

A.3.3. Conceptual Implication

Although the instantaneous time-dilation factor $1/a$ diverges (i.e., tends to infinity) as $a \to 0$, the observer-accumulated effective time remains finite. In this sense, the classical Big Bang singularity is approached only asymptotically within the EAoU framework and is never reached in finite accumulated observer-frame time. Instead, the Effective Age of the Universe converges toward a total duration of approximately 46 Gyr.

As a consequence, the cumulative contribution to the EAoU from the Big Bang up to recombination is

$$T_{\mathrm{eff}}\left(0 \to t_{\mathrm{rec}}\right) \approx 1\,\mathrm{Gyr},$$

which constitutes only a minor fraction (≈ 2 %) of the total Effective Age of the Universe.

As the scale factor $a \to 0$, the instantaneous time-dilation factor $1/a$ diverges, indicating that each emission-frame interval is increasingly stretched when mapped to the observer's frame. However, the proper-time intervals themselves shrink more rapidly ($\mathrm{d}t \propto a^2$), so the resulting observer-frame increments $\mathrm{d}T_{\mathrm{obs}} = \mathrm{d}t/a \propto a$ vanish. Consequently, the dilation rate diverges, but the proper-time intervals collapse sufficiently fast that the accumulated observer-frame time remains finite.

The time-dilation factor itself is defined as:

$$\mathrm{TDF} \equiv \mathrm{d}T_{\mathrm{obs}}/\mathrm{d}t$$

and diverges as $a \to 0$. This divergence refers to the *instantaneous mapping rate* between emission-frame and observer-frame time, not to the accumulated observer-frame duration. Although the dilation factor grows without bound, the corresponding observer-frame increment $\mathrm{d}T_{\mathrm{obs}} = \mathrm{d}t/a(t)$ vanishes because the proper-time intervals $\mathrm{d}t$ collapse more rapidly than the dilation factor increases.

In other words, the rate at which observer-time accumulates diverges, but the amount accumulated per interval shrinks to zero, so the total observer-frame time remains finite.

A.4. Divergent Time Dilation and the Vanishing of $\mathrm{d}T_{\mathrm{obs}}$ as $a \to 0$

A.4.1. Mathematical Behavior

The EAoU relation $\mathrm{d}T_{\mathrm{obs}} = \mathrm{d}t/a$ may appear divergent because $1/a \to \infty$ as $a \to 0$.

However, radiation-era proper time satisfies $\mathrm{d}t \propto a^2$, giving

$$\mathrm{d}T_{\mathrm{obs}} = \frac{\mathrm{d}t}{a} \propto a \to 0.$$

Thus:

- instantaneous dilation diverges,

- but integrated duration converges,
- and early-time contributions are very small.

This behavior mirrors a coordinate horizon: divergent rate, finite integral. Using Equation (A5),

$$T_{\text{eff}}\left(0\to a\right)=\frac{a}{H_0\sqrt{\Omega_r}},$$

(valid during radiation domination, $H\left(a\right)\simeq H_0\sqrt{\Omega_r}\,a^{-2}$) demonstrating linear convergence as $a\to 0$.

A.4.2. Transition: From Differential to Integrated Interpretation

The results of Appendix A.3 show that even extreme early epochs contribute only finite EAoU.

The radiation scaling $\mathrm{d}t\propto a^2$ ensures that $\mathrm{d}T_{\text{obs}}=\mathrm{d}t/a\propto a$ vanishes, and by recombination the accumulated effective time is only ~1 Gyr.

The early Universe thus acts as a region of steep instantaneous dilation but shallow **cumulative** duration in the observer frame.

A.5. Summary of Early-Universe Contributions to the EAoU

1. Radiation dynamics enforce

$$\rho\propto a^{-4},H\left(a\right)\propto a^{-2},\mathrm{d}t\propto a^2.$$

2. The EAoU integrand remains finite; Equation (A5) converges as $a\to 0$.
3. The early Universe contributes only ~1Gyr to the EAoU.
4. The post-recombination Universe contributes the remaining ~46Gyr.
5. The Big Bang acts as a **dilation horizon**—infinite instantaneous dilation but finite integrated age.